PREPARATION AND CHARACTERIZATION OF SURFACE ENHANCED RAMAN SCATTERING SUBSTRATE THROUGH ELECTRO DEPOSITION OF SILVER-PEDOT FILM ON ITO GLASS SURFACE

A THESIS SUBMITTED TO
THE GRADUATE SCHOOL OF NATURAL AND APPLIED SCIENCES
OF
MIDDLE EAST TECHNICAL UNIVERSITY

BY

ÜZEYİR DOĞAN

IN PARTIAL FULFILLMENT OF THE REQUIREMENTS
FOR
THE DEGREE OF MASTER OF SCIENCE
IN
CHEMISTRY

SEPTEMBER 2011

Approval of the Thesis;

PREPARATION AND CHARACTERIZATION OF SURFACE ENHANCED RAMAN SCATTERING SUBSTRATE THROUGH ELECTRO DEPOSITION OF SILVER-PEDOT FILM ON ITO GLASS SURFACE

submitted by **ÜZEYİR DOĞAN** in a partial fulfillment of the requirements for the degree of **Master of Science in Chemistry Department**, **Middle East Technical University** by

Prof. Dr. Canan Özgen
Dean, Graduate School of **Natural and Applied Sciences** ________________

Prof. Dr. İlker Özkan
Head of Department, **Chemistry** ________________

Prof Dr. Mürvet Volkan
Supervisor, **Chemistry Department, METU** ________________

Assoc. Prof. Dr. Atilla Cihaner
Co-Supervisor, **Chemical Engineering and** ________________
Applied Chemistry Dept., Atılım University

Examining Committee Members:

Prof. Dr. O. Yavuz Ataman
Chemistry Department, METU ________________

Prof. Dr. Mürvet Volkan
Chemistry Department, METU ________________

Prof. Dr. Necati Özkan
Polymer Science and Technology Department, METU ________________

Assoc. Prof. Dr. Nursen Çoruh
Chemistry Department, METU ________________

Assoc. Prof. Dr. Atilla Cihaner
Chemical Engineering and ________________
Applied Chemistry Dept., Atılım University

Date: 23.09.2011

I hereby declare that all information in this document has been obtained and presented in accordance with academic rules and ethical conduct. I also declare that, as required by these rules and conduct, I have fully cited and referenced all material and results that are not original to this work.

Name, Last name: Üzeyir DOĞAN

Signature:

ABSTRACT

PREPARATION AND CHARACTERIZATION OF SURFACE ENHANCED RAMAN SCATTERING SUBSTRATE THROUGH ELECTRO DEPOSITION OF SILVER-PEDOT FILM ON ITO GLASS SURFACE

Doğan, Üzeyir

M.Sc., Department of Chemistry
Supervisor: Prof. Dr. Mürvet Volkan
Co-supervisor: Assoc. Prof. Dr. Atilla Cihaner

September 2011, 69 pages

Detection of chemicals is a vital part of chemistry. For this reason, many detection systems are developed by scientists and every detection system has its own advantages. Raman spectroscopy is one of these detection systems having many advantages. However, this technique suffers from low signal intensity disadvantage. By developing a well prepared substrate, this problem can be easily solved; moreover, even single molecule detection can be possible.

In this study, a novel surface enhanced Raman scattering (SERS) substrate was prepared in two steps: In the first step, ethylenedioxythiophene (EDOT) monomer was polymerized electrochemically onto indium tin oxide (ITO) coated glass. In the next step, silver ions were reduced electrochemically onto surface prepared in the previous step.

In the substrate preparation part, the reduction potential of silver ion, the concentration of silver ions in solution, the polymer film thickness and reduced silver amount on substrates were optimized to get the best SERS performances from substrates. The prepared substrates were characterized by cyclic voltammetry (CV), ultraviolet-visible (UV-Vis) spectroscopy, scanning electron microscopy (SEM), and energy dispersive X-ray spectroscopy (EDX) attached to SEM.

In the SERS performance investigation part, homogeneity and the shelf life of the prepared silver-PEDOT substrates were tested. Homogeneity is very important in terms for the applications of Raman technique in quantitative analysis since most of the reported substrates are lack homogeneity consideration, our study will be an important contribution to the literature. The stability of the substrate was investigated for a period of one month. The very small change in the signal at the end of one month indicated that the substrate can be used even longer time with high efficiency. In all the studies, brilliant cresyl blue (BCB) is used as a model compound.

Some important Raman active chemicals, namely, rhodamine 6G (R6G) and 4-mercapto benzoic acid (4-MBA) were detected by using the prepared substrates.

Keywords: Raman spectroscopy, homogeneous and stable SERS substrate, electrochemically prepared SERS substrate, PEDOT, silver.

ÖZ

İTO CAM YÜZEYİNE ELEKTROKİMYASAL YOLLA KAPLANAN GÜMÜŞ-PEDOT FİLMİNİN HAZIRLANMASI, KARAKTERİZE EDİLMESİ VE YÜZEYDE GÜÇLENDİRİLMİŞ RAMAN SAÇILMASI SUBSTRATI OLARAK KULLANILMASI

Doğan, Üzeyir

Yüksek Lisans, Kimya Bölümü
Tez Yöneticisi: Prof. Dr. Mürvet Volkan
Ortak Tez Yöneticisi: Doç. Dr. Atilla Cihaner

Eylül 2011, 69 sayfa

Kimyasalların saptanması kimyanın çok önemli bir parçasıdır. Bu nedenle bilim adamları birçok saptama yöntemi geliştirmiştir ve her yöntemin kendine özgü avantajları vardır. Raman spektroskopisi birçok avantaja sahip olan saptama yöntemlerinden biridir. Buna rağmen, bu teknik düşük sinyal dezavantajından sıkıntı çekmektedir. İyi hazırlanmış substratlar geliştirilerek bu problem kolayca çözülebilmekte ve buna ek olarak, tek bir molekülün saptanması bile mümkün olabilmektedir.

Bu çalışmada, yeni bir yüzeyde güçlendirilmiş Raman saçılımı (SERS) substratı iki aşamada hazırlanmıştır. İlk aşamada, etilendioksitiyofen (EDOT) monomerleri elektrokimyasal olarak indiyum kalay oksit (ITO) kaplanmış cam yüzey üzerinde polimerleştirilmiştir. Bir sonraki aşamada, gümüş iyonları yine elektrokimyasal olarak ilk aşamada hazırlanmış olan yüzey üzerinde indirgenmiştir.

Substrat hazırlama bölümünde, substratlardan en yüksek sinyal yoğunluğu almak amacıyla gümüşün indirgenme potansiyeli, gümüş iyonları içeren çözeltinin derişimi, polimer film kalınlığı ve indirgenen gümüş miktarları optimize edilmiştir. Hazırlanan substratlar, döngülü voltametre (CV), morötesi-görünür bölge (UV-Vis) spektroskopisi, tarayıcı elektron mikroskopu (SEM) ve tarayıcı elektron mikroskobuna bağlanan enerji dağıtıcı X-ray spektroskopisi (EDX) ile karakterize edilmiştir.

SERS performansının araştırılması bölümünde, hazırlanan gümüş-PEDOT substratlarının homojenliği ve raf ömrü test edilmiştir. Homojenlik Raman tekniğinde nicel analizlerde çok önem arz etmektedir. Rapor edilen substratların çoğu homojen olmadığından bizim çalışmamız literatüre önemli bir katkı sağlayacaktır. Substratın dayanıklılığı bir ay süre için araştırılmıştır. Bir ay sonundaki sinyalde gözlenen küçük değişiklik, substratın daha uzun zamanlar yüksek verimlilikle kullanılabileceğini göstermiştir. Tüm çalışmalarda parlak krezil mavisi (BCB) model bileşik olarak kullanılmıştır.

Bazı önemli Raman aktif kimyasallar; rodamin 6G (R6G) ve 4-merkapto benzoik asit (4-MBA) hazırlanan yüzeyler kullanılarak saptanmıştır.

Anahtar Kelimeler: Raman spektroskopisi, homojen ve kararlı SERS substratı, elektrokimyasal yöntemle hazırlanmış SERS substratı, PEDOT, gümüş.

To my wife and parents

ACKNOWLEDGEMENTS

I would like thank to my supervisor Prof. Dr. Mürvet Volkan for her guidance, supports, encouragement and criticism during my whole study. She made me gain scientific way of thinking.

I would also like to thank to Assoc. Prof. Dr. Atilla Cihaner for his elegant comments and the opportunities he offered in his lab; I am also grateful to Prof. Dr. Ahmet M. Önal for allowing me to perform some parts of my experiments in his laboratory.

I thank Murat Kaya for his helps and ideas during my studies. I have learned many things from him. I also thank to Merve İçli-Özkut for her helps during my studies.

I would like to thank all C-50 members; Sezen Keser, Recep Yüksel, Dilek Ünal, Tuğbanur Aslan, Tacettin Öztürk and all other lab-mates for their helps, supports and friendships.

I thank to Emrah Yıldırım for his helps in solving of the problems and of course for his valuable friendship. I thank to Ataman's research group for their friendships, supports and helps.

I appreciate to my best friends Davut Çavdar, Burak Poyraz, Samet Nargül, Erhan Çiçek, Uğur Bilgin, Muhammed Avcı and Abdulmecit Gökçe for the unforgettable memories and adventures we experienced together.

I am grateful to Emrah Karahan and Hamza Turhan for their endless friendships.

My parents Hatice and İsa Doğan, and my sisters Rukiye and Dilek deserve my gratitude for their endless love and supports.

My special thanks and appreciations go to my dear wife Muazzez whose support, patience, love and trust make everything possible.

TABLE OF CONTENTS

LIST OF TABLES

TABLES

LIST OF FIGURES

FIGURES

LIST OF ABBREVIATIONS

BCB	Brilliant Cresyl Blue
CCD	Charge Coupled Device
CE	Counter Electrode
CM	Chemical Enhancement Mechanism
CPs	Conducting Polymers
CV	Cyclic Voltammetry
CV%	Coefficient of Variation
EDOT	3,4-Ethylene Dioxythiophene
EDX	Energy Dispersive X-ray
EF	Enhancement Factor
EM	Electromagnetic Enhancement Mechanism
ITO	Indium-tin oxide
LSPR	Localized Surface Plasmon Resonance
ORC	Oxidation-Reduction Cycles
PEDOT	Poly(3,4-ethylenedioxythiophene)
RE	Reference Electrode
SCE	Standard Calomel Electrode
SEM	Scanning Electron Microscope
SERS	Surface Enhanced Raman Scattering
SPEL	Spectroelectrochemical
SSEF	SERS Surface Enhancement Factor
R6G	Rhodamine 6G
UV-Vis	Ultraviolet Visible
WE	Working Electrode
4-MBA	4-Mercapto Benzoic Acid

CHAPTER 1

INTRODUCTION

1.1 Raman Spectroscopy

Infrared absorption and Raman scattering form the basis of main spectroscopic methods used to detect molecular vibrations. These methods provide information about the physical and chemical properties of the molecules since spectral patterns which are called fingerprinting of the molecules are detected with these methods. Moreover, quantitative determination of the substance in a sample can be also accomplished by these spectroscopic methods (Smith & Denth, 2005).

Raman and infrared spectroscopies are complementary. The spectral lines in the Raman spectroscopy show the vibrational modes of molecular bonds. These spectral lines depend on the net change in the polarizability, not the change in dipole moment (McCreery & Richard, 2000). The change in dipole moments is required for infrared spectroscopy, and this change results from electron density shift upon vibration in the molecule. On the other hand, disturbance of the electron distribution around a bond causes the polarization which is needed for Raman spectroscopy (Jeanmarie & Van Duyne, 1977). This polarization results in inelastic scattering of monochromatic light which is measured by Raman spectroscopy (Princeton Instruments). Sir Chandrasekhara Venkata Raman discovered what is called the “Raman effect” in 1928 which made him win the Nobel Prize in 1930 (Venkata Raman - Biography); (Long, 2002).

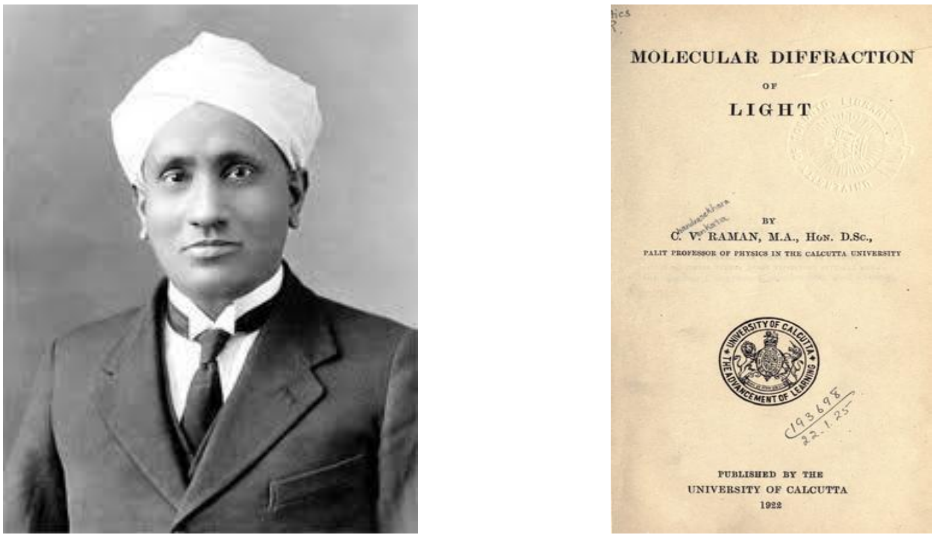

MOLECULAR DIFFRACTION
OF
LIGHT
BY
C. V. RAMAN, M.A., Hon. D.Sc.,
PALIT PROFESSOR OF PHYSICS IN THE CALCUTTA UNIVERSITY

PUBLISHED BY THE
UNIVERSITY OF CALCUTTA
1922

Figure 1.1 Indian scientist Sir C.V. Raman and cover page of his study rewarded with Nobel Prize (Saagam); (Open Library).

1.1.1 Raman scattering

1.1.1.1 History of Raman Scattering

In 1923 Smekal hypothesized on the phenomenon of inelastic scattering of light (Smekal, 1923). This hypothesis was experimented and conformed by Chandrasekhara Venkata Raman and Kariamanickam Srinivasa Krishnan in 1928 (Raman & Krishnan, 1928). The sample in the experiment was either purified liquid or dust free vapor on which sunlight was focused using a telescope. The scattered radiation coming from the sample was collected by an additional lens. In order to prove the presence of scattered radiation having a changed frequency from the descendent light, the researchers employed a system of optical filters. The existence of this phenomenon was called the Raman effect afterwards. On account of this discovery and contribution to the scattering of light, Raman was rewarded with the Nobel Prize in Physics in 1930 (Venkata Raman - Biography). The significance of this discovery was proved on December 15, 1998 by the American Chemical Society and the Indian Association for the Cultivation of Science designating the Raman effect as International Historic Chemical Landmark (ACS).

1.1.1.2 Theory of Raman Scattering

Upon the interaction of monochromatic light with the matter, the photons may either be absorbed by the matter or scattered from it, or they may pass through it. The photons are absorbed when their energies correspond to the energy gap between the ground and excited state of the molecule. Absorption spectroscopy measures this energy change of the photons. However, the photons may also be scattered from the molecule when they interact with it. In this case, it is not necessary for the incident photons to have an energy corresponding to the energy gap between ground and excited states of the molecule. In the case of scattering of light from the molecule, molecular energy level goes up to a virtual level from the ground state. The virtual state results from the distortion of the electron cloud around the nuclei by the coming monochromatic light whose frequency determines the energy level of this state since the virtual state is not stable, the photons are re-radiated quickly (Smith & Denth, 2005). If the energies of the incident light and the scattered light are the same, this is called elastic scattering or Rayleigh scattering. On the other hand, if the energies of the incident and scattered light are different, this is called inelastic scattering or Raman scattering (Figure 1.2). Rayleigh scattering is the dominant one as discovered by Sir Raman and Sir Krishnan since one in a million photons is scattered inelastically (Stevenson & Vo-Dinh, 1996).

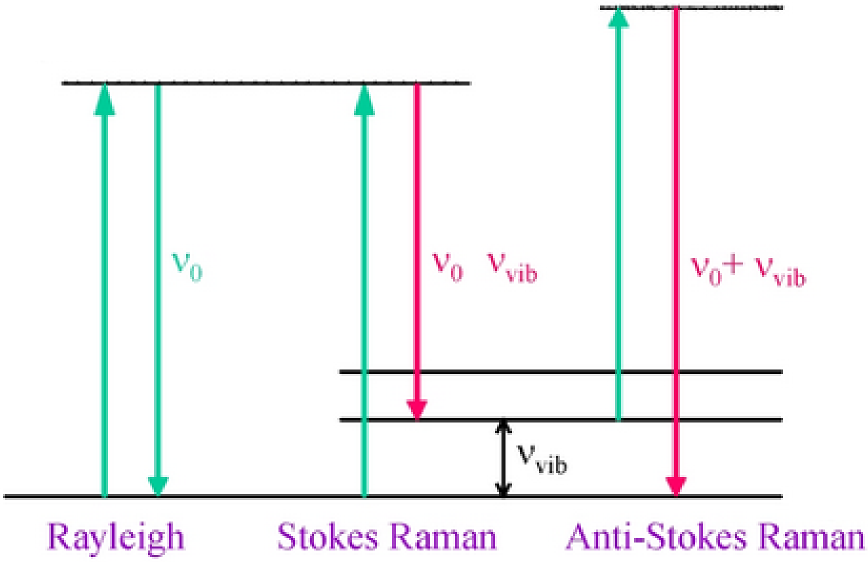

Figure 1.2 Rayleigh and Raman scattering energy diagram (Vrije Universiteit).

Raman scattering may take place in two ways: Stokes Raman scattering and anti-Stokes Raman scattering (Figure 1.2). When the energy of the incident photon is higher than the scattered photon, then Stokes Raman scattering occurs. When the vice versa condition is the case, anti-Stokes Raman scattering takes place. The population of the various states of the molecule determines the relative intensities of these two processes since most molecules are in their ground energy states at room temperature according to the Boltzmann equation, Stokes scattering is dominant compared to anti-Stokes scattering. However, rising the temperature will increase anti-Stokes scattering, since at higher temperatures more molecules will be at their higher energy levels. The difference between Stokes and anti-Stokes scattering can also be used to calculate temperature (Smith & Denth, 2005).

Figure 1.3 shows typical spectrum of Stokes, anti-Stokes and Rayleigh scattering from cyclohexane, a commonly used Raman standard. Rayleigh scattering is seen at zero, which is the most intense peak. The system is at thermal equilibrium with its environment; thus, Stokes lines have much intense signals than the anti-Stokes lines.

The bands for Stokes and anti-Stokes are represented as wavenumber in cm^{-1}, showing the gain or loss of energy from the incident light (Movasaghi, Rehman, & Rehman, 2007). This energy difference is termed as the Raman shift, which is unique for most of the molecules.

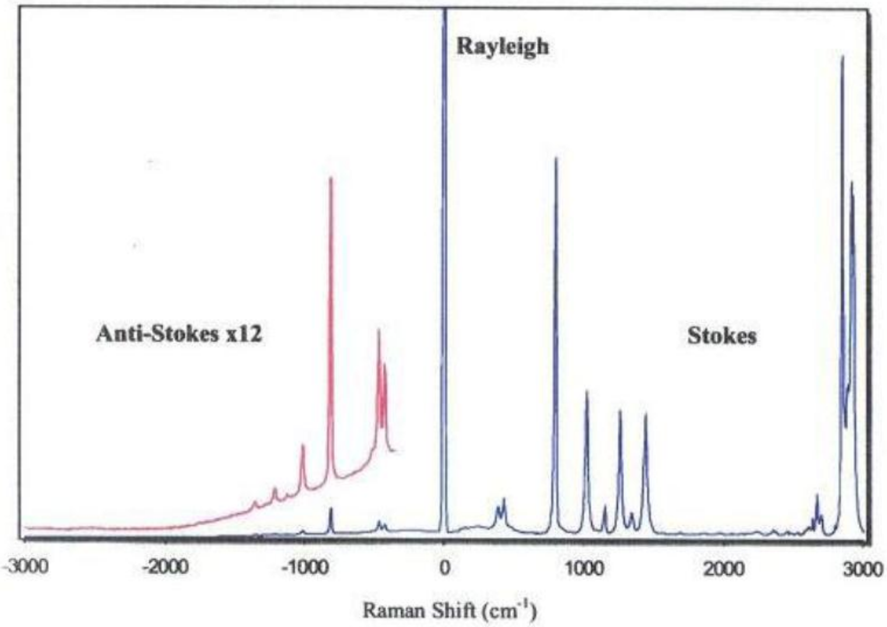

Figure 1.3 Raman spectrum of cyclohexane **(**Smith & Denth**,** 2005**)**; (College of Chemistry).

Stokes scatterings records are usually given in Raman spectrum; while sometimes anti-Stokes may be preferred in the case of some interference, such as fluorescence. Since fluorescence interference occurs at a lower energy than the excitation frequency and consequently anti-Stokes scattering can be used (Smith & Denth, 2005).

The Raman shift does not depend on the wavelength of the coming light. The Raman shift can be calculated using the following equation (Strobel & Heineman, 1989).

$$\Delta v = \frac{1}{\lambda_I} - \frac{1}{\lambda_O}$$

The $\Delta \upsilon$ in equation is the observed Raman shift. The wavelength of the coming light is shown by λ_I and the wavelength of the scattered light is shown by λ_O. The greater the wavelength of the incident light, the larger the shift in wavelength is expected to be. However, no change is observed in the energy shift (Strobel & Heineman, 1989).

Raman scattering is a very rare process as stated above, one in a million scattering process. This causes a problem in terms of low sensitivity and leading loss of detectability of most of the molecules with Raman spectroscopy. This problem was overcome by developing surface enhanced Raman scattering (SERS) technique.

1.1.2 Surface Enhanced Raman Scattering

The low intensity problem of Raman scattering was solved by the discovery of SERS. This technique not only enhanced the surface sensitivity, but also leaded the detection of many chemicals. This made Raman spectroscopy more useful as a detection tool in various applications.

Efficient Raman scattering was first observed by Fleischmann et al. from pyridine molecules which are adsorbed on silver electrode surfaces (Fleischmanna, Hendraa, & McQuillana, 1974). It was suggested that roughening process made more pyridine molecules to be adsorbed on the surface since the electrode surface area was increased. However, two other groups proved that the increase in the signal intensity was not because of the increase in the surface area, since if it was due to the roughened surface, the enhancement would be less than a factor of 10, while the observed signal intensity was 10^6 orders of magnitude. (Jeanmarie & Van Duyne, 1977; Albrecht & Creighton, 1977). Jeanmaire and Van Duyne proposed electromagnetic enhancement mechanism (EM) whereas Albrecht and Creighton proposed chemical enhancement mechanism (CM). Parts of each proposed mechanisms, were in fact, correct. Therefore, SERS enhancement results from contributions of these two mechanisms (Stiles, Dieringer, Shah, & Van Duyne, 2008). Over the years, the surface enhancement has been attributed to these two different mechanisms.

1.1.2.1 Electromagnetic Enhancement Mechanism

In order to better understand the EM, localized surface plasmon resonance (LSPR) should be mentioned first since it is responsible for EM. The interaction of a monochromatic light with a metallic nanoparticle results in displacement of the conduction electron cloud (Figure 1.4). The collective excitation of this electron cloud of a conductor near surface region called as surface plasmon. The presence of surface plasmons was first predicted by Ritchie (Ritchie, 1957). The incident light causes excitation of the surface plasmons around the nanometer sized metallic structures which is called LSPR. A molecule present in LSPR field produces more intense Raman scattering than molecules outside the field. The enhancement of the Raman scattering strongly depends on size, shape, the organization of the particles in clusters, and the frequency of the incident light (Jain, Huang, & El-Sayed, 2007; Germain, Brioude, Ingert, & Pileni, 2005). When the wavelength of the coming monochromatic light is close to LSPR of metallic surface, the molecules adsorbed to the surface or close to the surface cause a large electromagnetic field. Thus, this large electromagnetic field enhances the Raman signal more (Campion & Kambhampati, 1998); (Orendorff, Gearheart, Jana, & Murphy, 2006).

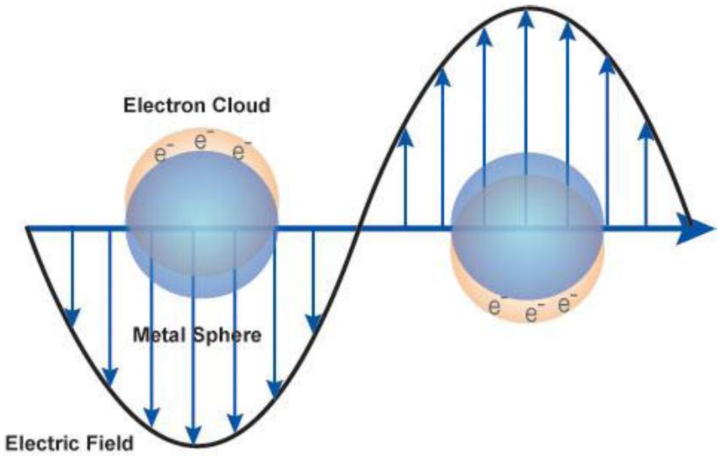

Figure 1.4 A schematic representation of surface plasmons confined to a spherical metal surface.

Surface plasmon resonance results from oscillations of the conduction electrons in the metal surface when an external electric field causes excitation of these electrons. SERS makes use of the interaction of coming laser with the surface plasmon on the metal surface which causes electromagnetic enhancement. SERS occurs in five steps. The coming light at a certain angle excites a surface plasmon first. Then, in the second step, the molecules on the surface are polarized by the large electric field of plasmons; thus, effective and large dipole moments occur between the molecules. Molecular polarization changes if a molecule changes its vibrational state in this situation. Next, a new plasmon surface field is formed upon the change in polarization. At the last step, the surface plasmon can couple into an outgoing Raman scattered photon. The distances more than atomic size characterize the EM, which is independent from specific molecule-metal interaction on the surface and adsorption properties of the molecules. That is why the SERS spectra and Raman spectra of free molecules do not differ when the EM is operative.

1.1.2.2 Chemical Enhancement Mechanism

CM, also called as charge transfer, is based on the formation of a bond between the metal surface and the analyte, which produces surface species, composed of surface atoms and analyte (Otto, Mrozek, Grabhorn, & Akemann, 1992). Thus, charge transfer from the metal to the analyte becomes possible. The interaction of the metal electrons with the molecule induces polarizability of the molecule. The bond between the metal surface and the analyte forms new electronic states which are thought to be resonant intermediates in Raman scattering. On the contrary to the surface plasmons through which light is absorbed or scattered, the metal absorbs the radiation. After the excitation of the metal atoms, re-radiation occurs from the metal surface.

There are evidences for both of the mechanisms and it is difficult to differentiate them. For the CM to proceed, only monolayer should be formed on the surface since the enhancement occurs only form the surface bound molecules. On the other hand, the range of effect of EM is larger, but it decreases with the $1/r^3$ distance from the surface. Still, the highest EM occurs on monolayer coverage on the surface. Both mechanisms increase Raman scattering. Having enhancement of 10^5-10^7 times compared to Raman scattering, EM is suggested to contribute more to total enhancement than CM does, which enhances the Raman scattering 10^1-10^2 times (Campion, Ivanecky, Child, & Foster, 1995).

The mechanisms become multiplicative when both the chemical and electromagnetic mechanisms contribute to the system (Campion & Kambhampati, 1998). In this case the overall enhancement factor (EF) of the system can be estimated by using the following formula (Murphy C. J., et al., 2008).

$$EF = \frac{\frac{SERS\ Intensity}{\#\ of\ molecules}}{\frac{Raman\ Intensity}{\#\ of\ molecules}}$$

The integration time must be taken into consideration in the calculation of the enhancement factor (Murphy C. J., et al., 2008). The number of excited molecules is affected by beam dimensions and incident surface power; therefore, these parameters should be considered in the comparison of SERS and Raman intensities. Taking these additional parameters into consideration, the SERS surface enhancement factor (SSEF) can be calculated with the below formula (Le Ru, Blackie, & Etchegoin, 2007).

$$SSEF = \frac{\frac{I_{SERS}}{\mu_M \mu_S A_M}}{\frac{I_{RS}}{C_{RS} H_{eff}}}$$

I_{SERS} and I_{RS} are the SERS and normal Raman intensities, respectively, in the equation above. The surface density of the individual nanostructures is represented by μ_M and μ_S represents the surface density of the molecules on the substrate surface. A_M is the area of the metallic surface, while the concentration of the solution is shown by C_{RS}. Finally, H_{eff} is the effective height of the scattering volume. Up to 10^{14} enhancement factors were observed, this means the detections of even a single molecule. Kneipp et al. and Nie et al. have reported that under favorable conditions it is possible to detect single molecule based on its SERS spectra (Kneipp, et al., 1998; Kneipp, Kneipp, Deinum, Itzkan, Dasari, & Feld, 1998); (Kneipp, Kneipp, Itzkan, Dasari, & Feld, 1999; Kneipp, Kneipp, Manoharan, Itzkan, Dasari, & Feld, 1998); (Kneipp, et al., 1997); (Nie & Emory, 1997; Maxwell, Emory, & Nie, 2001).

1.1.3 SERS Substrates

Surface Enhanced Raman Spectroscopy required the employment of SERS active substrate. The substrate should be composed of the coinage metals (silver, gold and copper, etc.) since they support surface plasmons, leading increase in the signal intensities (Siemes, Bruckbauer, Goussev, Otto, Sinther, & Pucci, 2001); (Lu, Ruan, Yang, Xu, Zhao, & Zhao, 2008); (Liu Y. , 2004). Among the coinage metals, silver provides the greatest enhancement in most of the reported studies (Arunkumar & Bradley, 1983).

Many different methods have been developed in order to prepare SERS active substrates during the past decades. The SERS active substrates can be prepared by using one of the following methods:

- Preparation of solutions of colloidal metal nanoparticles
- Deposition of metal particles on surfaces using different physical techniques (vapor deposition, photodeposition, vacuum evaporation, thermal evaporation)
- Acid etching of metal foils
- Laser-ablation of metal plates
- Electrochemically prepared metal surfaces

Colloidal solution, the most commonly used enhancement substrate with high enhancement performance and simple preparation (Sanci & Volkan, 2009); (Vongsvivut, Robertsona, & McNaughtona, 2010). It has been shown that the shape, size, geometry, alignment, and proximity of nanostructures can greatly influence the SERS enhancement (El-Sayed, Nikoobakht, & Mostafa, 2003); (Duan, Cai, Luo, Li, & Li, 2006). However, in most studies results were lack of reproducibility of signals, suffering from aggregation of metallic nanoparticles. Attaching nanoparticles to a supporting substrate is one of the alternative ways to overcome the shortcomings of colloidal substrates (Vo-Dinh, 1998); (Freeman, et al., 1995); (Park, Yoon, & Kim, 2006). Furthermore, by using SERS substrates based on ordered template, the stability, uniformity, and reproducibility of SERS substrates can be further improved.

Deposition of metal particles is a good technique, especially for preparing uniform and reproducible SERS substrates (Christou, Knorr, Ihlemann, Wackerbarth, & Beushausen, 2010). However, the instruments needed to deposition of metal particles with different methods are generally very expensive instruments.

Acid etched metal foils also used as SERS substrate (Rupérez & Laserna, 1996). Prepared substrates with this method also suffer from uniformity and reproducibility of SERS substrates. In addition, the signal enhancement factor values of these substrates relatively small compared with substrates prepared by using other techniques.

SERS substrates prepared by using laser ablation technique are also used (Lee, Han, & Kim, 2001). However, need for a laser and difficulties in the substrate preparation part also make this technique less practical as compared with other techniques.

SERS technique was firstly discovered on substrate which was roughened silver electrode surface. After this discovery, many groups prepared substrates by using electrochemical method (Vosgröne, Meixner, Anders, Dietz, Sandman, & Plieth, 2004); (Yang, Liu, Hsu, & Juang, 2009); (Liu, Yu, & Sheu, 2006). Recently, a controllable and reproduced surface roughness can be generated through control of the electrochemical oxidation-reduction cycles (ORC) procedure (Chuang, Liu, & Thomas, 2003).

It can be clearly stated that, there is no any ideal substrate for all SERS applications. All research groups prepare or develop their own SERS substrates by considering their needs and facilities.

1.1.4 Instrumentation of Raman Spectroscopy

A Raman spectrometer is composed of a laser source, a sample illumination system, a wavelength selector, and transducer with a readout system. The diagram of the Raman spectrometer is shown in Figure 1.5.

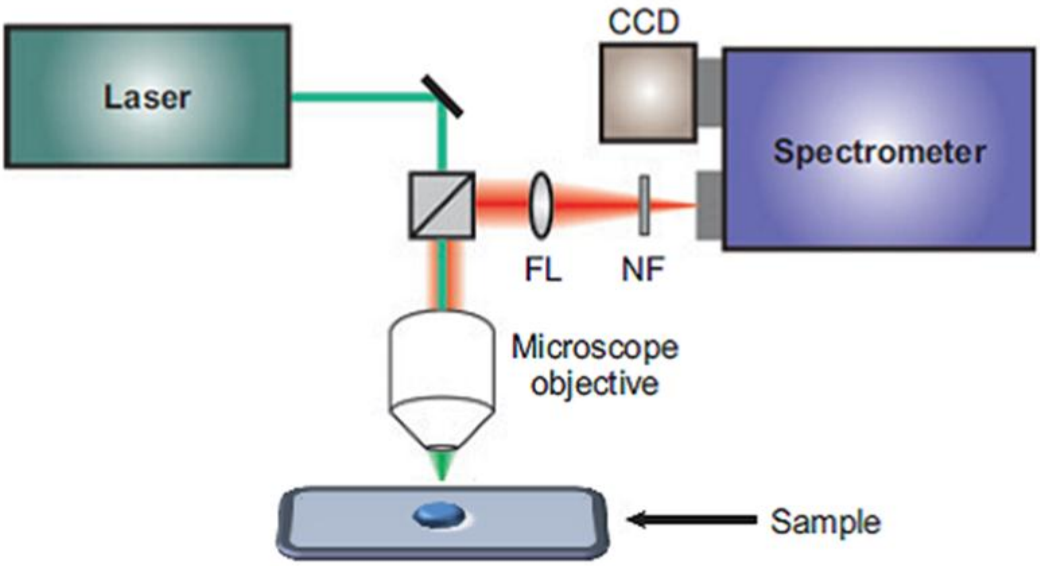

Figure 1.5 Schematic representation of Raman spectroscopy.

1.1.4.1 Source

The source used in Raman spectrometer is almost always lasers since the high intensity of laser is required to produce sufficient Raman scattering. Some common laser sources used in Raman spectroscopy are listed in Table 1.1. Ar^+ lasers emit light at 488.0 and 514.5 nm, while Kr^+ lasers emit at 530.9 and 647.1 nm. Since the intensity of Raman scattering increases as the forth power of frequency of the laser, argon and krypton ion sources that emit light in the blue and the green region of the spectrum, have an advantage over the other laser sources. For instance, the argon ion laser at 488.0 nm provides three times more intense Raman signals compared to He-

Ne source emits light at 632.8 nm, when given the same input power (Skoog, Holler, & Nieman, 1998). Diode and Nd/YAG laser sources carry an advantage over the laser sources having shorter wavelength. The first advantage is the opportunity of usage of high power up to 50 W without causing photodecomposition of the analyte. The second one is having low energy which prevents fluorescence interference for most of the molecules. The selection of the laser source should be optimized so that Raman signals should be intense as much as possible, photodecomposition of the sample and fluorescence interference should be as low as possible (Ingle & Crouch, 1988).

Table 1.1 Some common laser sources for Raman spectroscopy.

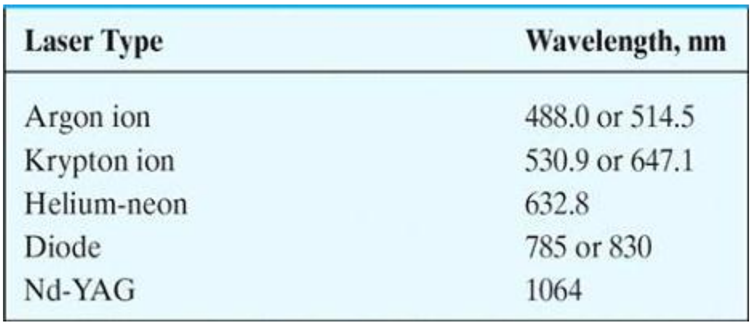

Laser Type	Wavelength, nm
Argon ion	488.0 or 514.5
Krypton ion	530.9 or 647.1
Helium-neon	632.8
Diode	785 or 830
Nd-YAG	1064

1.1.4.2 Sample Illumination System

Raman spectroscopic measurements are simple since glass can be used as sample holder, instead of the more fragile and atmospherically less stable crystalline halides. Laser source can be easily focused on a small area of sample; therefore, a small amount of samples can be examined. There are different types of sample holders enabling investigation of solid, liquid, and gas samples.

1.1.4.3 Wavelength Selector

The wavelength selector carries a high importance in Raman spectrometer. In order for the weaker Raman lines to be separated and eliminated from the intense Rayleigh lines coming from the sample, holographic interference filters, called notch filters, or a monochromator are usually used. For the improvement of the resolution of the Raman spectrum multiple monochromators can be utilized (Ingle & Crouch, 1988).

1.1.4.4 Transducer and Readout System

Historically, photomultiplier tubes were used as detectors in Raman spectrometers (Ingle & Crouch, 1988). Recently, most Raman spectrometers include Fourier transform instruments equipped with cooled germanium transducers or charge coupled devises (CCD) based detectors. The selection of the detector system depends on the sample’s fluorescence interference. There is a conflict on the better detector system whether it is Fourier transform instruments or CCD based detectors.

1.1.5 Applications of Raman Spectroscopy

Raman spectroscopy can be used in wide range applications in chemistry. It can be utilized in the detection of biological molecules like proteins, bacteria, oligonucleotides and nucleic acids. Furthermore, biomolecular interactions like antibody/antigen interaction and streptavidin/biotin interactions can be detected by Raman spectroscopy. Besides the detection of adenosine, glucose, some toxic ions such as lead, mercury and cadmium have been detected by Raman spectroscopy with ligand based nanoparticles. Therefore, this method can be applied in pharmaceuticals, as well as in forensic sciences. Raman spectroscopy can also be used in the detection of organic, inorganic species and polymeric materials. This makes it a useful tool in many areas.

1.1.6 Advantages of Raman Spectroscopy

The Raman spectroscopy has many advantages. One of the advantages is the usage of water and other polar solvents which do not appear in the Raman spectra. Moreover, glass can be used in the parts of the Raman spectrometer instrument because Raman spectrometer commonly utilizes the light in the visible and near-IR range (Skoog, Holler, & Nieman, 1998). Since the laser can be directly focused on the sample, no sample preparation is necessary. Raman spectroscopy gives more detailed information related with the chemical structure of the scattering molecule compared with most of the other detection techniques.

1.2 Conducting Polymers

Today, the polymers are very important due to frequently usage in the supplementation of human needs. Among them, conducting polymers (CPs) attract attention for being used in variety of technological applications such as photovoltaics (Liscio, De Luca, Nolde, Palermo, Müllen, & Samori, 2008), transistors (Usta, Facchetti, & Marks, 2008), light-emitting diodes (Goel, et al., 2008) and molecular electronics (Chen, et al., 2008).

The first study conducted on CPs was reported by Shirakawa, MacDiarmid and Heeger in 1977 (Chiang, et al., 1977; Chiang, Park, Heeger, Shirakawa, Louis, & A.G., 1978). They discovered highly conducting iodine-doped polyacetylene, which brought them the Nobel Prize in chemistry in 2000. After the discovery of first conducting polymer, a new research area was born. Many CPs have been developed and their properties have examined during the last three decades. Some commonly used CPs are listed below consisting of polypyrrole (Diaz, Kanazawa, & Gardini, 1979), polyfuran (Gandini & Belgancem, 1997), polythiophene (Tourillon & Garnier, 1982), poly(3,4-ethylenedioxythiophene) (PEDOT) (Jonas & Schrader, 1991), polyaniline (MacDiarmid & Epstein, 1989), poly(p-phenylenevinylene)

(Burroughes, et al., 1990), and polycarbazole (Desbene-Monvernay, Lacaze, & Dubois, 1981).

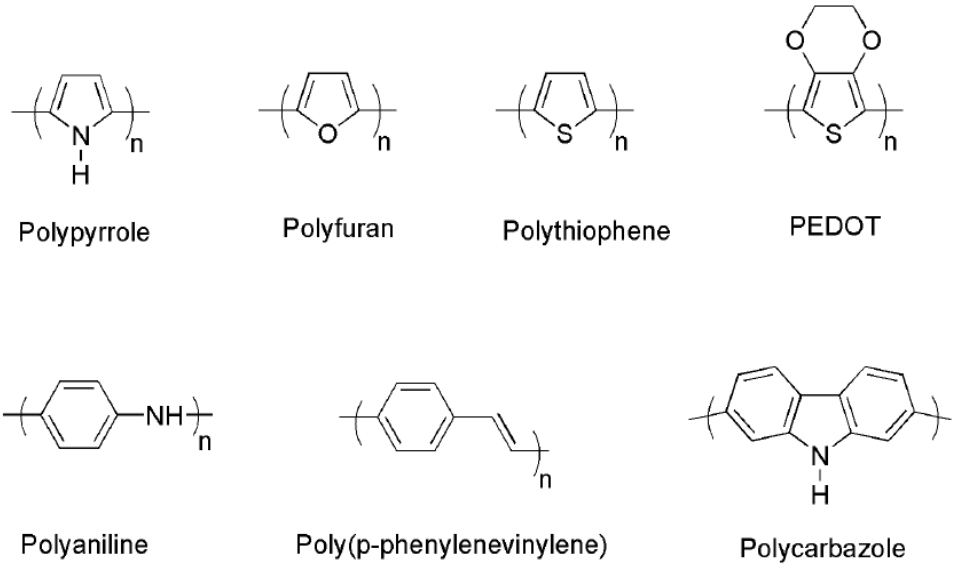

Polypyrrole

Polyfuran

Polythiophene

PEDOT

Polyaniline

Poly(p-phenylenevinylene)

Polycarbazole

Figure 1.6 Some commonly used conducting polymers.

1.2.1 Synthesis of Conducting Polymers

Synthesis of CPs can be achieved either by chemical or electrochemical polymerization. The choice of the polymerization technique mainly depends on the usage area of the resultant polymer. For instance, electrochemical polymerization method is useful when the main aim is to obtain polymer with desired amount, since the polymer amount can be adjusted via counting the charge passing during the polymerization. Usually, small amounts of monomer can be polymerized by using electrochemical polymerization method. On the other hand, chemical polymerization method is more convenient way if the large amounts of compound are desired (Inzelt, 2008).

1.2.1.1 Electrochemical Polymerization

When potential is applied to working electrode, upon oxidation of monomer present in electrolytic medium, reactive radical cations are formed, which forms the basis of electrochemical polymerization. By one of the two subsequent ways, the polymer is formed. In the first one, oxidation of the radical cation-neutral monomer couple makes the couple to lose two protons; thus, a neutral dimer is formed (Asavapiriyonont, Chandler, Pletcher, & Gunawardena, 1984). In the second way, the neutral dimer is formed upon the loss of two protons of the coupling of two radical cations (Genius, Bidan, & Diaz, 1983). Then, oxidation of dimer and repetition of coupling process take place. The dimer has lower potential than monomer; thus, its oxidation of it becomes easier. The electroactive polymer deposits on the working electrode with the process of chain length increase. Figure 1.7 shows the general mechanism of polymerization of heterocycles.

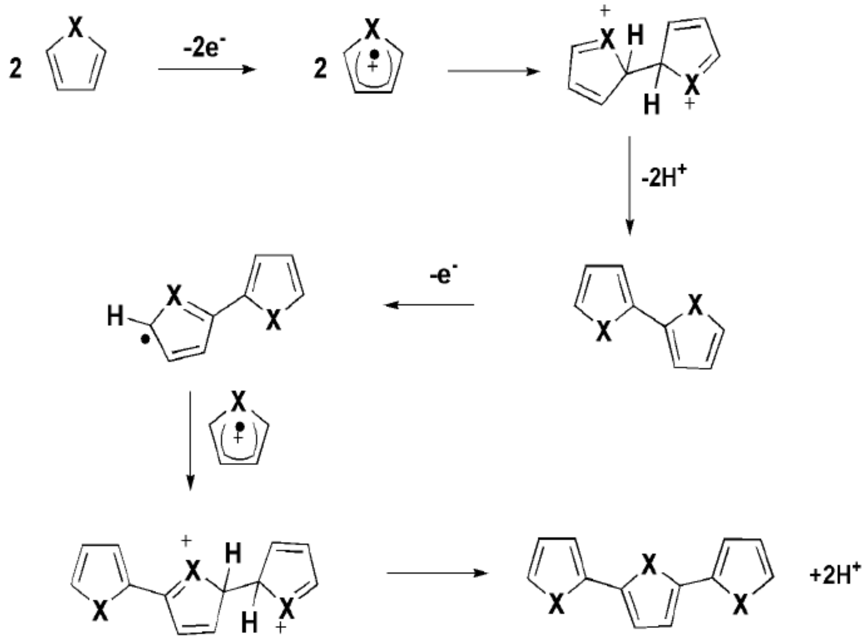

Figure 1.7 Electropolymerization mechanism of heterocyclic monomers (X = S, O, NH)) (Gaupp, 2002).

The advantages of electrochemical polymerizations can be listed as follows:

- The necessary amount of monomer is low.
- The polymers are acquired in a short time.
- In situ analysis is possible with this polymerization method.
- Controlling the applied potential eliminates the side reactions.
- By changing scan rate, time and the applied potential, the conductivity and the thickness of polymer film can be controlled.

The polymerization efficiency is affected by the stability of resultant radical cations. The removal of the electrons from the monomer is easy, which also affects the polymerization efficiency. Indeed, it is harder for the electron poor monomers to lose an electron than for the electron rich monomers. Electron rich monomers, by the resonance across π-electron system, make the resultant radical cations more stable (Figure 1.8).

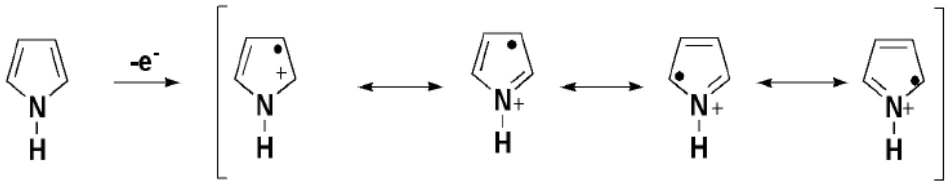

Figure 1.8 Radical cation stability of pyrrole monomer.

As shown in Figure 1.9 together with α-α’ coupling, α-β couplings may occur. By α-β couplings, polymers with different parts having distinct electronic features and conductivity are generated; thus, polymer homogeneity is harmed. α-β, β-β linkages are eliminated by replacement of hydrogen atoms of 3- and 4- positions of monomers with alkoxy and alkyl groups in EDOT monomers.

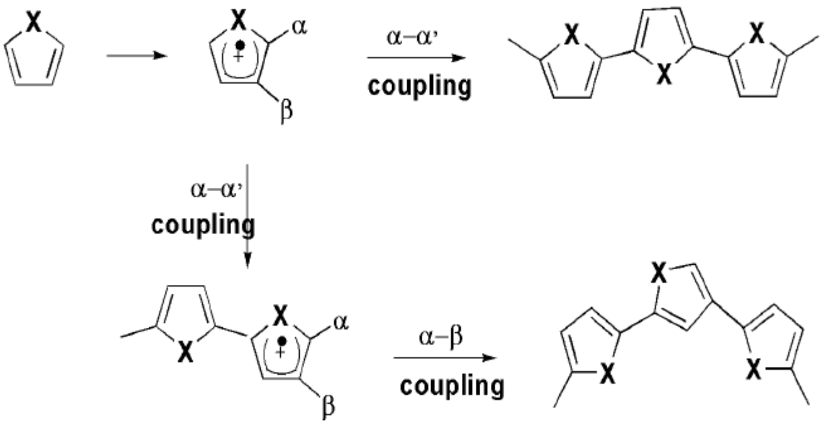

Figure 1.9 Possible α-α’ and α-β couplings of unsubstituted heterocylic monomers (X = S, O, NH) (Gaupp, 2002).

Electrochemical cells can be used in electrochemical polymerization. These cells should have three electrodes compared with classical ones which have two electrodes; a working and a reference electrode or two working electrodes since the potential difference measurement is the aim. On the other hand, three electrodes are used in electrochemical polymerization. As shown in Figure 1.10, these electrodes are working electrode (WE), reference electrode (RE) and counter (auxiliary) electrode (CE). The voltage difference between WE and RE is monitored but the current between CE and WE is measured during measurement.

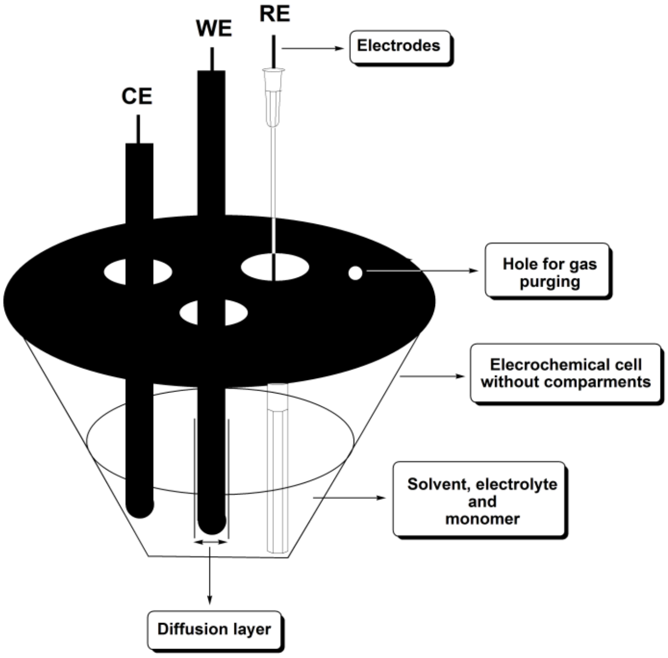

Figure 1.10 Representation of an electrochemical cell used for electrochemical polymerization and/or analysis (İçli Özkut, 2011).

The monomer type, aim of the study and stability of polymer on the electrode surface determine the type of WE. A steel electrode is used in corrosion studies, for instance. As being transparent, ITO coated glass is chosen when the aim is the spectroelectrochemical (SPEL) analysis of polymers. ITO coated glass is used since ITO coating provides electrical conductivity on the surface of glass to be used as an electrode. Gold, platinum and glassy carbon electrodes are also preferable when WE is needed to be inert in the study.

In most of the studies, platinum is preferred as the CE. The important point in the selection of CE is that CE should have larger surface area than WE whose mass control via migration should be eliminated.

For the reference electrode, Ag wires, standard calomel electrodes (SCE) and Ag/AgCl are often used.

For obtaining the electrochemical polymerization in a desired way, the selection of the solvent and the supporting electrolyte are very crucial.

1.2.1.1.1 Solvent

As stated above, choice of solvent is very important for electrochemical polymerization. First of all, it should dissolve the monomer but not the polymer which forms on the surface of WE. This characteristic may not be obtained always from the one type of solvent. In this case, solvent mixtures are used to gain these properties.

One another parameter that should be taken into account when selecting the solvent is the working range, which is the potential window. Table 1.2 shows some of the commonly used solvents for electrochemical polymerization and their working ranges.

Table 1.2 Some commonly used solvents and their working potential ranges (Wise, Wnek, Trantolo, Cooper, & Gresser, 1998).

Solvent	**Approximate Working Range (V) vs. SCE**
Acetonitrile (ACN)	+2.7 to -3.2
N,N-Dimethyl formamide (DMF)	+2.0 to -1.8
Propylene carbonate (PC)	+2.0 to -2.0
Dichloromethane (DCM)	+1.8 to -1.7
Water	+1.1 to -0.8

1.2.1.1.2 Supporting Electrolyte

Electrochemical reaction occurs around 3-8 A^o of the working electrode in an electrochemical cell. This layer is called diffusion layer (Figure 1.10). The access of the monomers to the diffusion layer occurs by mass transfer which takes place in three ways; diffusion, migration and convection. In fact, during electrochemical polymerization and/or voltammetric analysis, the process should be only diffusion controlled, according to Randles-Sevcik equation shown below.

$$i_p = kn^{3/2}AC(VD)^{1/2}$$

where i_p is peak current, k is a constant, n is the number of electrons transferred, A is electrode area in cm^2, C is concentration in mole/mL, V is the scan rate in V/s, D is diffusion coefficient in cm^2/s.

To eliminate convection, mixing is avoided and to eliminate migration, supporting electrolyte is used. Besides to eliminate the migration, the supporting electrolytes are used as a counter ion in doping process. The type of the counter ion affects the growth rate of the polymer film on the electrode surface. It also affects the morphology of the polymer formed. For example, BF_4^- or ClO_4^- containing polyanilines have more compact structure than Cl^- or NO_3^- containing ones (Inzelt, 2008).

The frequently used electrolytes are tetrabutylammonium hexafluorophosphate (TBAH), tetrabutylammonium tetrafluoroborate ($TBABF_4$), lithium perchlorate ($LiClO_4$), potassium chloride (KCl) and potassium nitrate (KNO_3).

1.2.2 Poly(3,4-ethylenedioxythiophene)

The first CPs have problematic electronic properties which limit the electrosynthesis. In order to overcome this problem, PEDOT was produced following the polymerization of EDOT (Figure 1.9). The β-positions were blocked by the cyclic ethylenedioxy bridge and this blockage provides only α-α' coupling during polymerization process. This is the reason of regular polymerization of EDOT. This property is very crucial in our studies to get homogeneous surfaces.

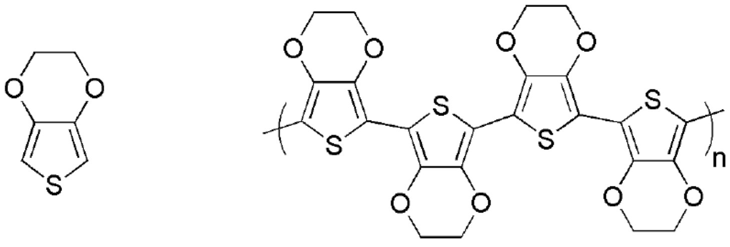

Figure 1.11 Structure of EDOT and PEDOT

1.2.3 Cyclic Voltammetry

CV is an electro analytical technique which is widely used for synthesis and characterization of CPs. It has a simple usage which makes it a preferable technique. In this technique, the current flow between working and counter electrodes is monitored as a function of the applied potential. During the CV cycles, the CPs deposit on the working electrode and decays its monomers with the changing applied potential. By looking the CV voltammograms, the oxidation and the reduction potentials of the polymer can be determined.

1.3 Aim of the Study

In this study, a new SERS active substrate using electrochemical method was prepared. The effect of substrate preparation parameters on SERS sensitivity was investigated and optimized. These parameters are silver reduction potential, silver ion concentration of solution, polymer film thickness and silver amounts on the substrates. Additionally, the homogeneity of the prepared substrates and stability of the substrates were examined in terms of its SERS activity by using low concentrations of BCB. Finally, prepared substrates are used to detect low concentrations of R6G and 4-MBA.

CHAPTER 2

EXPERIMENTAL

2.1 Materials

3,4-ethylenedioxythiophene, brilliant cresyl blue and 4-mercaptobenzoic acid were purchased from Aldrich. Rhodamine 6-G was purchased from Sigma. Silver nitrate ($AgNO_3$) was purchased from Merck. Lithium perchlorate ($LiClO_4$) was purchased from Acros Organics. Acetonitrile (ACN) was purchased from J. T. Baker. Indium tin oxide coated glass was purchased from Delta Technologies Co. Ltd., Stillwater. All reagents were in analytical grade and used without further purification. Aqueous solutions were prepared using 18 MΩ.cm deionized water obtained from a Millipore (Molsheim, France) Milli-Q water purification system.

2.2 Instrumentation

For the electrochemical studies, a Gamry PCI4/300 and Reference 600 potentiostat-galvanostat were used. A standard three-electrode setup was used in which Ag wire was used as a reference electrode, Pt wire was used as a counter electrode and ITO coated glass was used as a working electrode.

SERS measurements were performed with Jobin Yvon LabRam confocal microscopy Raman spectrometer with a charge-coupled device (CCD) detector and a holographic notch filter. The spectrograph was equipped with a 1800-grooves/mm grating and all

measurements were done with a 200 μm entrance slit. SERS excitation was provided by 632.8 nm radiation from a He-Ne laser with a total power of 20 mW.
SEM measurements were carried out with a ZEISS EVO LS15- Bruker Quantax electron microscope.

EDX was performed with a scanning electron microscope equipped with energy-dispersive X-ray analyzer.

UV-Vis spectra were collected over the range 370-800 nm by using double beam instrument Varian Cary 100. Quartz cells were used in all measurements.

2.3 Preparation of ITO-PEDOT-Ag Substrate

2.3.1 Electrochemical Polymerization of PEDOT on ITO Glass

0.1 M $LiClO_4$ solution was prepared in acetonitrile and filled into a quartz cell up to 2 cm level from the bottom of cell since the area of coated glass is important for optimization studies. Then, EDOT monomer concentration was adjusted to $1.0x10^{-2}$ M with the help of micropipette and pipetting up and down is done for the homogenous mixing of EDOT monomer into solution.

ITO coated glass was washed with acetone, and then placed into three electrode system which was placed into a quartz cell (Figure 2.1). After necessary connections were made, 1.5 V was applied to this electrolysis cell by using computer program of the instrument. By doing this, desired amounts of PEDOT were coated onto working electrode. Then, PEDOT coated ITO glass was washed with acetonitrile to remove the monomer and oligomeric species from the surface.

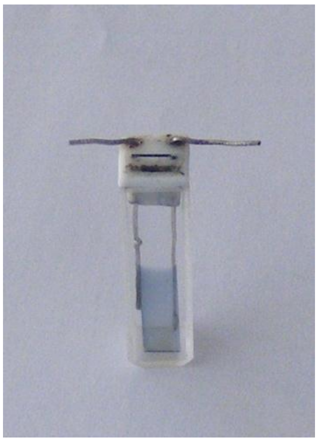

Figure 2.1 The picture of three electrode system.

To get the best SERS performance, PEDOT charge densities on the substrates were optimized by taking Raman measurements of BCB dye onto prepared substrates.

2.3.2 Electrochemical Reduction of Silver onto PEDOT Coated ITO Glass

$AgNO_3$ solutions were prepared in different concentrations in 0.1 M $LiClO_4$ dissolved acetonitrile solution. These solutions were filled into different quartz cells having 2 cm solution height since the area of reduced silver on glass is important for optimization studies.

Three-electrode system was placed into this quartz cell. After necessary connections were made, different voltage values were applied to this electrolysis cell by using computer program of instrument to reduce desired amounts of silver ions. Then, silver reduced PEDOT coated ITO glass was washed with acetonitrile to remove silver ions, lithium and perchlorate ions from the surface.

To obtain the best SERS performance, silver charge densities on the substrates, silver reduction potential and silver ion concentrations were optimized by taking CV measurements in appropriate solutions and Raman measurements of BCB dye onto prepared substrates.

2.4 Optimization of Parameters for Good SERS Performance

2.4.1 Optimization of Silver Reduction Potential

Initially, the critical potential value that can reduce silver ions was found by taking CV measurements. Then, reduction potential values of silver ions were varied to: -0.2, -0.3, -0.4, -0.5 V, and CV measurements were taken for different silver amounts. Using the appropriate reduction potentials determined from CV measurements, various substrates were prepared and their SERS performances were investigated.

2.4.2 Optimization of Silver Ion Concentration

The concentrations of solution containing silver ions were varied: 1.0×10^{-3}, 2.0×10^{-3}, 5.0×10^{-3}, 1.0×10^{-2} M. Using these solutions having different concentrations, various substrates were prepared and their CV behaviors and SERS performances were investigated.

2.4.3 Optimization of PEDOT Film Thickness and Silver Amount

The optimization was carried out by allowing deposition of PEDOT and silver at various charge densities on the surfaces. Table 2.1 shows the charge densities trials for PEDOT and silver. The SERS performances of substrates having different PEDOT and silver charge densities were investigated.

Table 2.1 The amounts of the polymer and silver deposited.

Polymer Amount (mC/cm^2)	Silver Amount (mC/cm^2)
10	10
20	30
30	40
	50
	60
	70

2.5 Tests to Show Usability of Substrates

2.5.1 Homogeneity Test

SERS measurements of BCB were taken on different points of the prepared substrate to test the homogeneity of the substrate. Four different points were determined on the same substrate and many measurements were taken at these points.

2.5.2 Stability Test

SERS measurements of BCB were taken at different times on the same surface to test the stability of the substrate. The taken measurements were on the 1st, 7th, 14th, and 28th days after preparation.

2.6 SERS Studies

The performance of SERS active substrates was evaluated by using R6G and 4-MBA Raman active molecules. Solutions of these analytes were prepared in ethanol for both chemicals with different concentrations to be used for serial dilutions.

Those Raman active molecules were dropped onto prepared substrates as shown in Figure 2.2 and Raman measurements were taken at a range of wavenumber with 1000-2000 cm^{-1} for both chemicals.

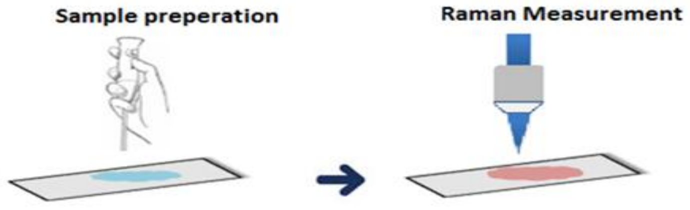

Figure 2.2 Schematic representation of SERS measurements.

CHAPTER 3

RESULTS AND DISCUSSION

In the present study, for the first time, a new SERS active substrate was prepared by using PEDOT polymer and used for the detection of some important Raman active chemicals. PEDOT polymer provides a highly homogeneous surface for SERS applications. This homogeneity for SERS active substrates is very critical for quantitative applications. In addition, prepared substrates provide really high SERS signal enhancements about 10^5 orders of magnitude. In order to prepare this highly SERS active substrate, many optimizations were performed. Silver reduction potential, silver ion concentrations of solution in which silver reduction takes place, PEDOT and silver charge densities on substrates, were optimized by the help of CV and SERS techniques. Then, to show substrate usability, homogeneity and stability of substrates were investigated. In these optimization studies, BCB is used as a model compound. SERS efficiency of prepared substrates was measured by using R6G and 4-MBA. The characterizations of prepared substrates were done by using CV, SEM, EDX, and UV-Vis spectroscopy.

3.1 ITO-PEDOT-Ag Substrate Preparation

In this substrate preparation section, PEDOT was coated electrochemically on ITO glass surface before the silver reduction. Substrate preparation using electrochemical methods has started with one of our former group members, Bahar Köksel (Köksel, 2009). She worked on SERS substrate composed of electrochemically reduced silver particles onto polymer poly-1,22-bis(1,1-pyrrole)-3,6,9-trioxaundecane. The prepared substrates have shown really high SERS signal enhancements and they have been used successfully in the detection of trace amount of nicotinic acid and nicotine. However, the same SERS enhancement for the analytes could not be obtained at the every point of the prepared substrate due to inhomogeneous reduction of silver ions onto polymer. In this study instead of poly-1,22-bis(1,1-pyrole)-3,6,9-trioxaundecane, PEDOT polymer was used and similar to Köksel’s study, silver ions reduced onto the polymer by using electrochemical reduction method.

3.1.1 Preparation of PEDOT Coated ITO Glass Substrate

EDOT monomer was polymerized electrochemically at 1.5 V vs. Ag wire in 0.1 M $LiClO_4$ in acetonitrile electrochemically. A blue film coated on the surface of ITO glass was an indication of the formation of PEDOT polymer at the end of electrochemical polymerization process (Figure 3.1).

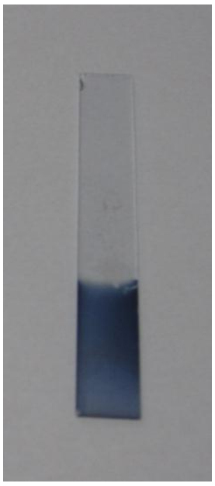

Figure 3.1 The picture of PEDOT coated ITO glass.

The thickness of polymer film deposited on ITO glass during the electrochemical polymerization of EDOT can be increased by extending the duration of the electrochemical polymerization, resulting in an increase in the charge density of PEDOT polymer film on the working electrode.

In order to confirm PEDOT polymer film formation on the ITO glass surface, the redox behavior of the obtained polymer was taken in a monomer free electrolytic solution containing 0.1 M $LiClO_4$ in acetonitrile (Figure 3.2).

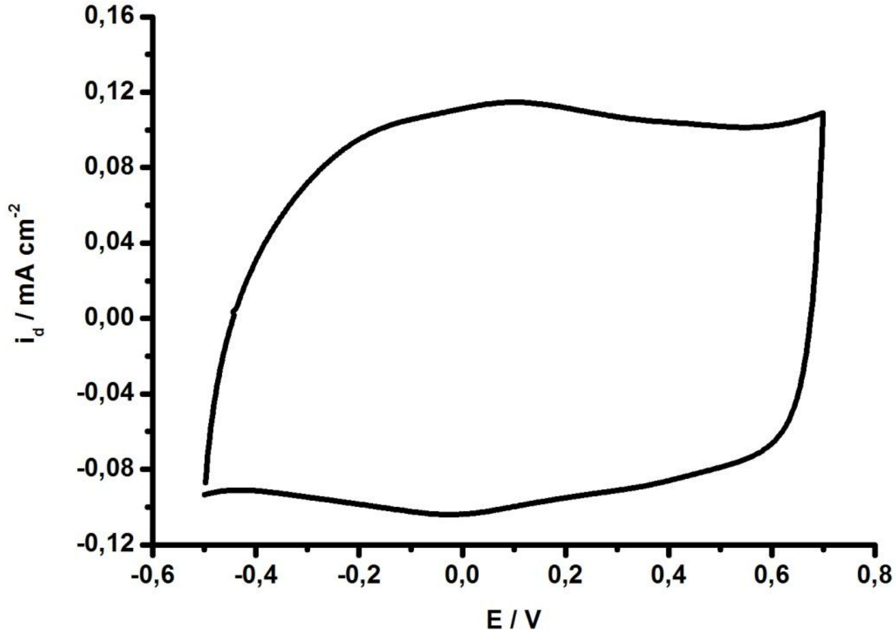

Figure 3.2 Cyclic voltammogram of PEDOT film on an ITO electrode in 0.1 M $LiClO_4$ solution in acetonitrile at 50 mV/s.

Figure 3.2 shows a typical cyclic voltammogram of PEDOT polymer which indicates the coating of the polymer on ITO electrode.

3.1.2 Silver Reduction onto PEDOT Coated ITO Glass Substrate

Silver was reduced onto polymer film electrochemically by applying -0.2 V vs. Ag wire in 2.0×10^{-3} M $AgNO_3$ in 0.1 M $LiClO_4$/acetonitrile solution. Gray color indicates the formation of silver particles onto the surface of the blue PEDOT film at the end of electrochemical reduction process (Figure 3.3.b).

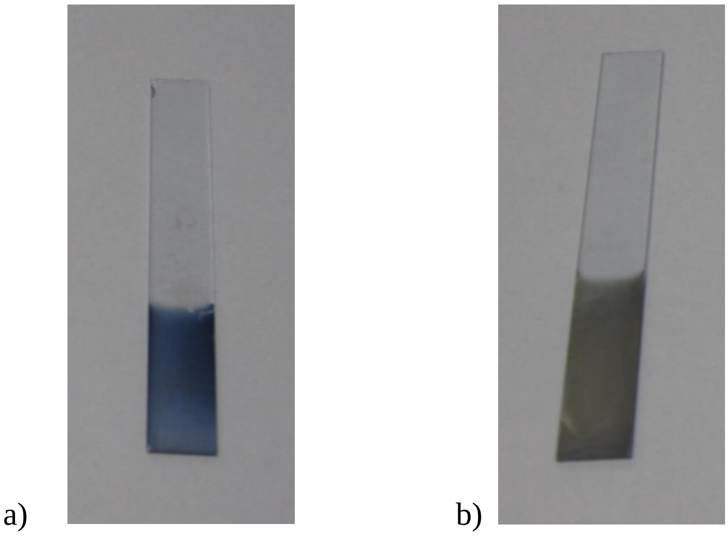

Figure 3.3 a) PEDOT coated ITO glass **b)** Silver reduced on PEDOT coated ITO glass.

UV-Vis absorption spectrum of silver doped PEDOT film on ITO glass is shown in Figure 3.4. Absorption peak at 485 nm shows the evidence of silver particles; however, the peak is red shifted compared with the absorption maxima of regular silver nanoparticles which is located at 420 nm (Yin, Li, Zhong, Gates, Xia, & Venkateswaran, 2002). The reasons of this phenomenon are the size of silver particles (around 900 nm) and the interaction between PEDOT polymer and silver particles.

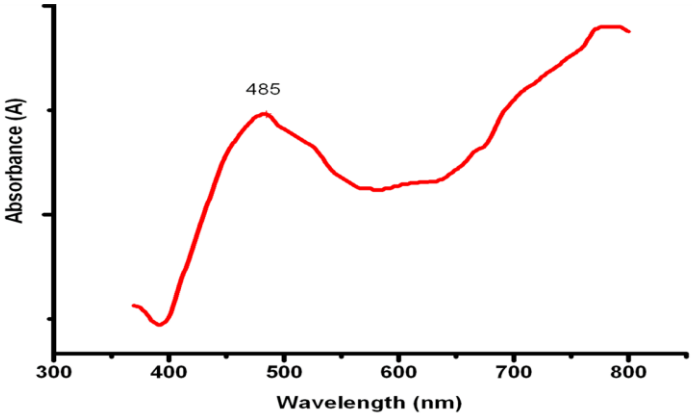

Figure 3.4 UV-Vis spectrum of silver-PEDOT film on ITO.

SEM image of electrochemically reduced silver particles on PEDOT film is shown in Figure 3.5. From the SEM image, it is seen that nanometer sized silver islands formed on PEDOT film homogeneously. These silver structures are primarily responsible for the SERS enhancement as well as reproducible SERS signal measurements.

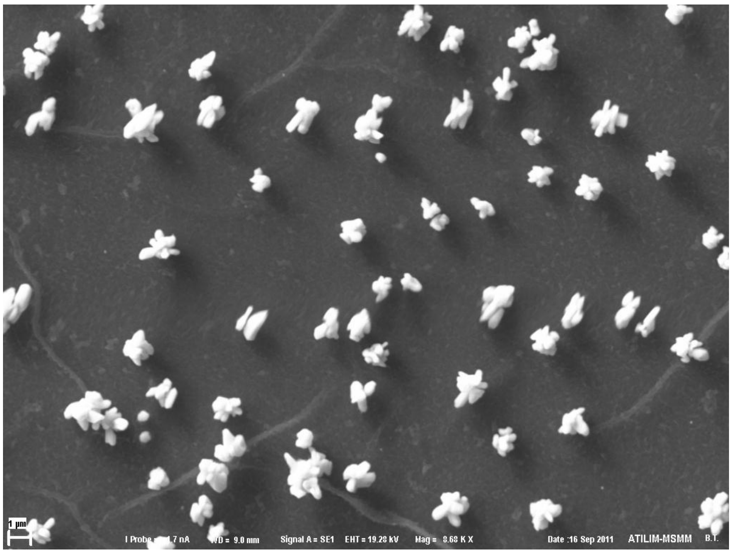

Figure 3.5 SEM image of silver-PEDOT film on ITO.

EDX measurements of substrates also prove the presence of silver metal (Figure 3.6).

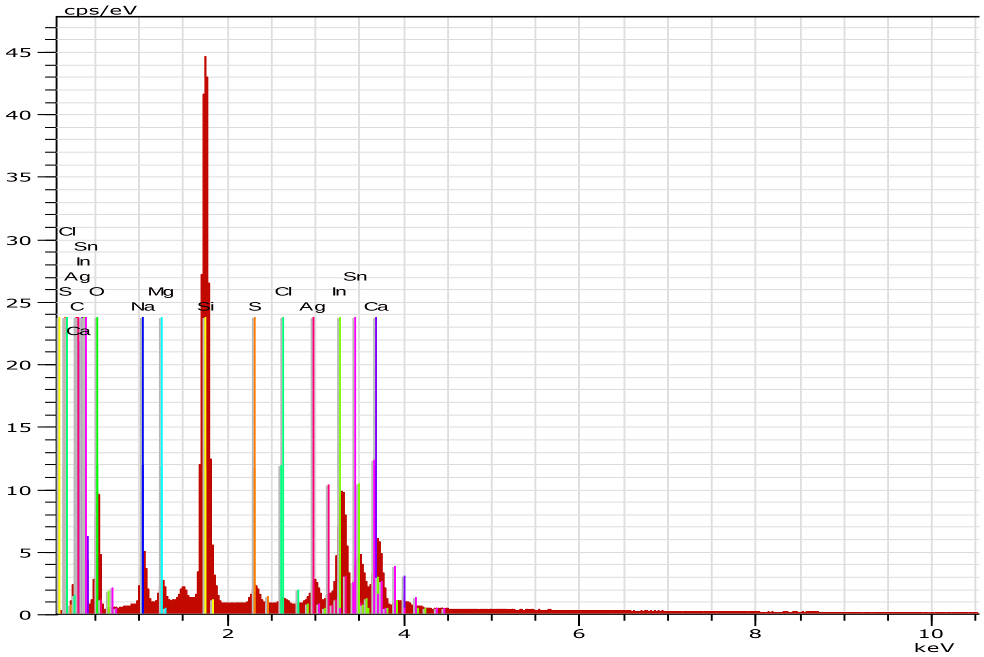

Figure 3.6 EDX measurement of silver reduced substrate.

3.2 Optimization of Substrate Preparation Parameters for Good SERS Performance

The parameters that will be discussed in this section are reduction potential of silver, silver ion concentration of solution where silver reduction was performed, PEDOT polymer film thickness on the working electrode, and the amount of silver particle on the polymer film. These optimizations were evaluated by considering the outcomes of the SERS and CV measurements of the substrates. In other words, many substrates were prepared by changing parameters and optimum value was decided by analyzing the SERS spectra and/or CV cycles of the substrates.

3.2.1 Optimization of Reduction Potential of Silver

The effect of the reduction potential of silver on reduction was examined by CV measurements continuing to six different potentials shown in Figure 3.7. Silver reduction was not taking place when CV measurement continued to 0.0 V but very small amount of silver could be reduced when CV measurement continued to -0.1 V (Figure 3.8).

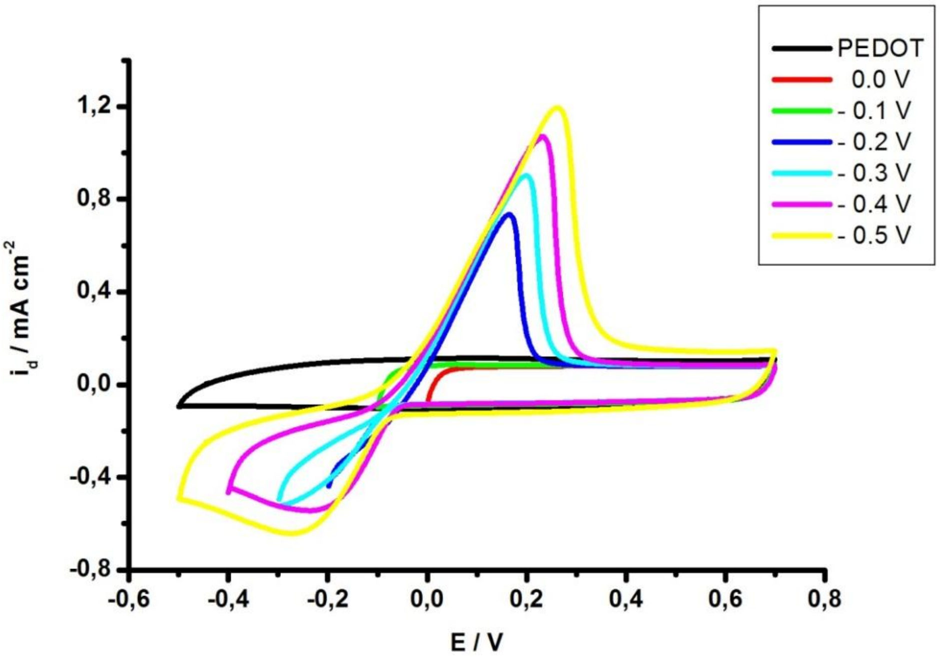

Figure 3.7 CV measurements of substrates continue to different voltage values in 0.002 M $AgNO_3$ dissolved in 0.1 M $LiClO_4$/ACN at 50 mV/s vs. Ag wire.

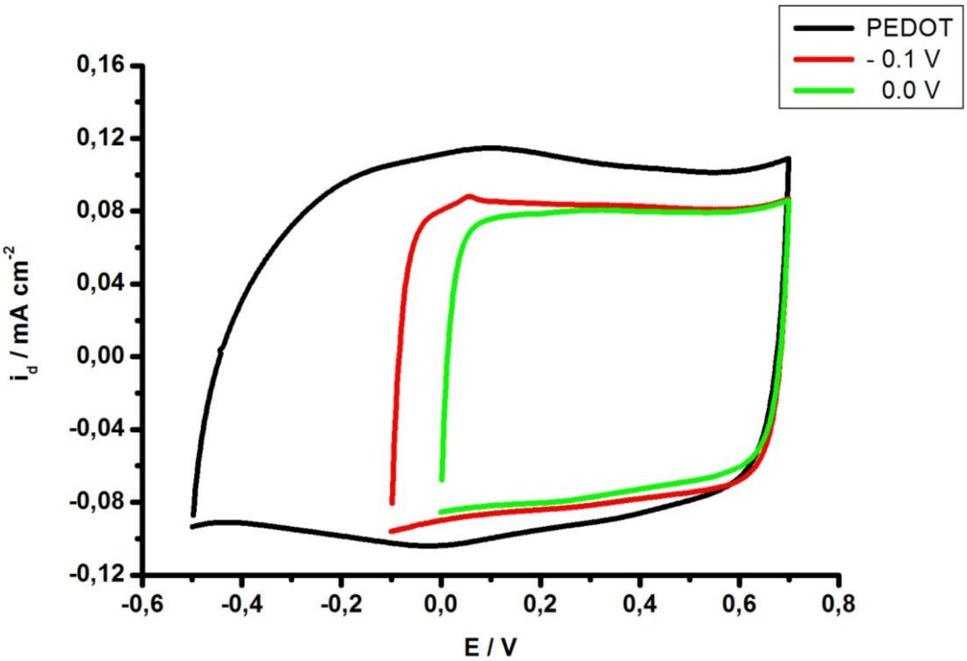

Figure 3.8 CV measurements of substrates continue to 0.0 V and -0.1 V voltage values in 0.002 M $AgNO_3$ dissolved in 0.1 M $LiClO_4$/ACN at 50 mV/s vs. Ag wire.

In Figure 3.7 and Figure 3.8, the CV measurements of PEDOT were also shown together with other CV measurements. These CV measurements of PEDOT were taken in the absence of silver ions. Therefore, silver reduction and silver oxidation peaks were not observed.

More accurate optimization of silver reduction potential can be determined by looking at different silver amounts at different voltages. The Figure 3.7 and Figure 3.8 show that, silver reduction clearly starts at -0.2 V. Therefore, potentials from -0.2 V to -0.5 V were scanned to determine the optimum silver reduction potential. This optimum value was also confirmed by SERS measurements.

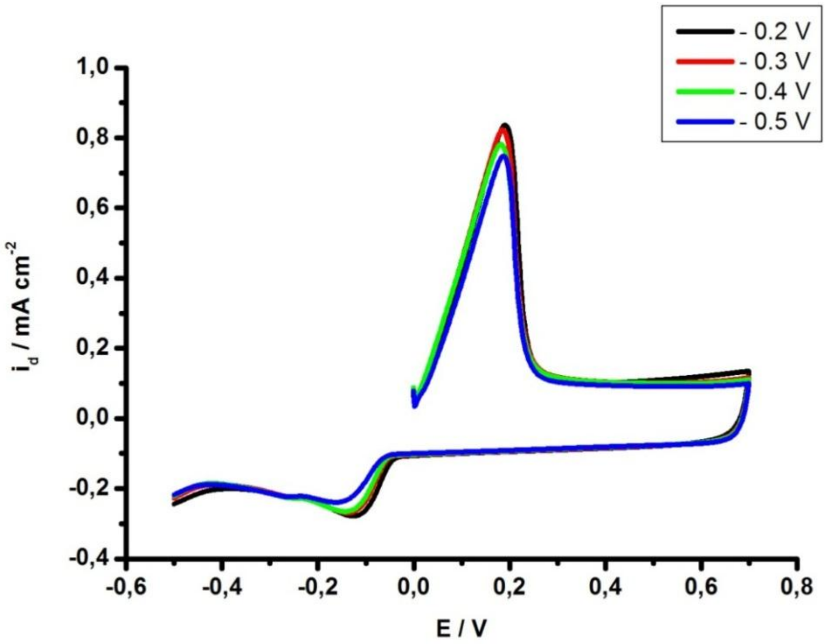

Figure 3.9 CV measurements of substrate having 2.5 mC/cm^{-2} silver charge density in 0.1 M $LiClO_4$ dissolved in ACN at 50 mV/s vs. Ag wire.

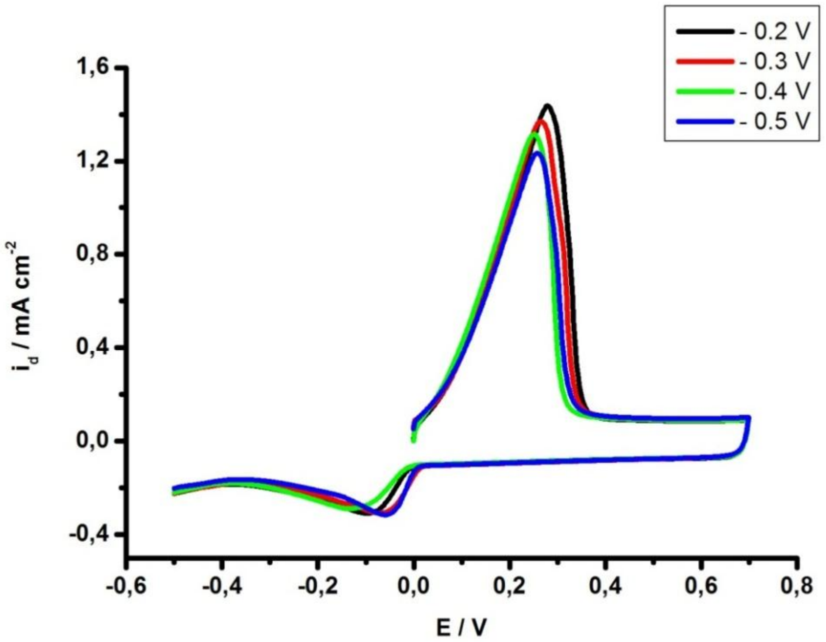

Figure 3.10 CV measurements of substrate having 5 mC/cm^{-2} silver charge density in 0.1 M $LiClO_4$ dissolved in ACN at 50 mV/s vs. Ag wire.

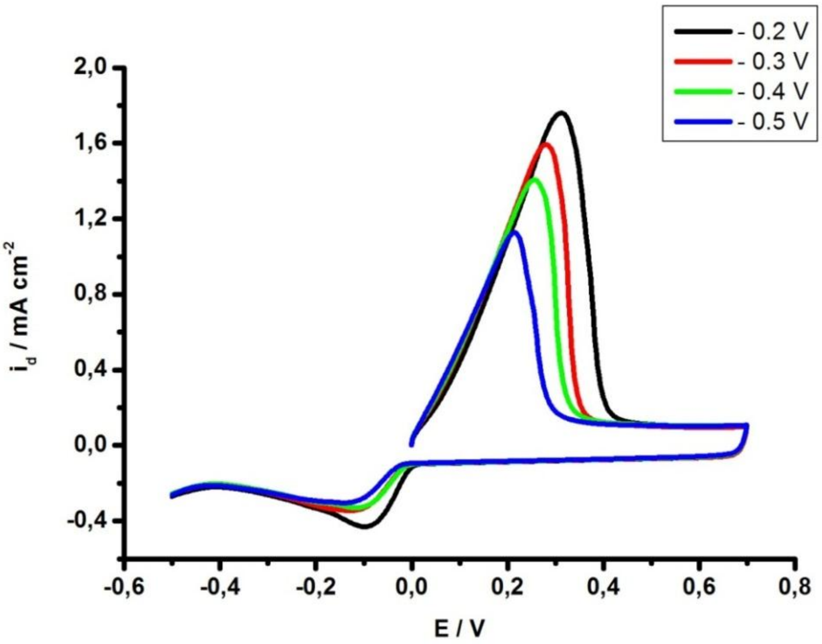

Figure 3.11 CV measurements of substrate having 7.5 mC/cm^{-2} silver charge density in 0.1 M $LiClO_4$ dissolved in ACN at 50 mV/s vs. Ag wire.

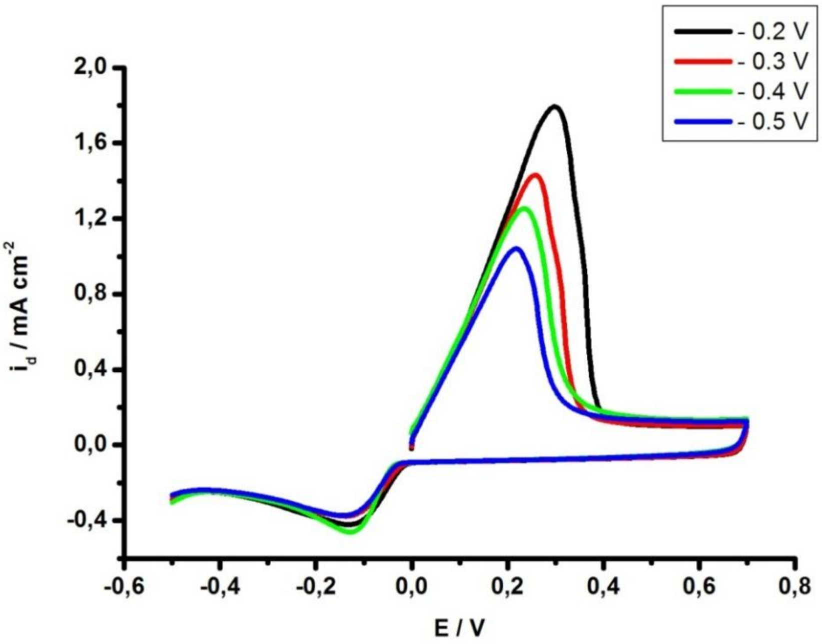

Figure 3.12 CV measurements of having 10 mC/cm^{-2} silver charge density in 0.1 M $LiClO_4$ dissolved in ACN at 50 mV/s vs. Ag wire.

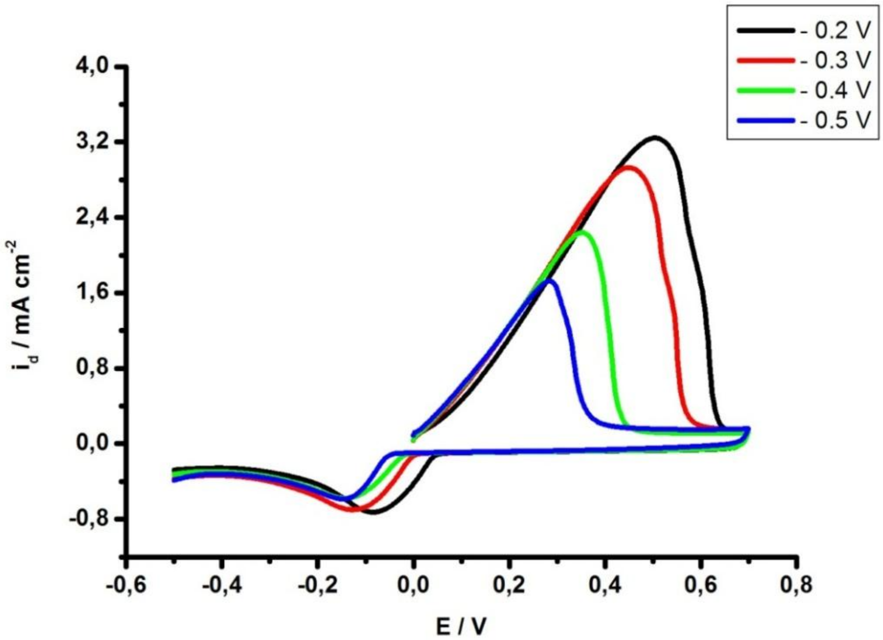

Figure 3.13 CV measurements of substrate having 25 mC/cm^{-2} silver charge density in 0.1 M $LiClO_4$ dissolved in ACN at 50 mV/s vs. Ag wire.

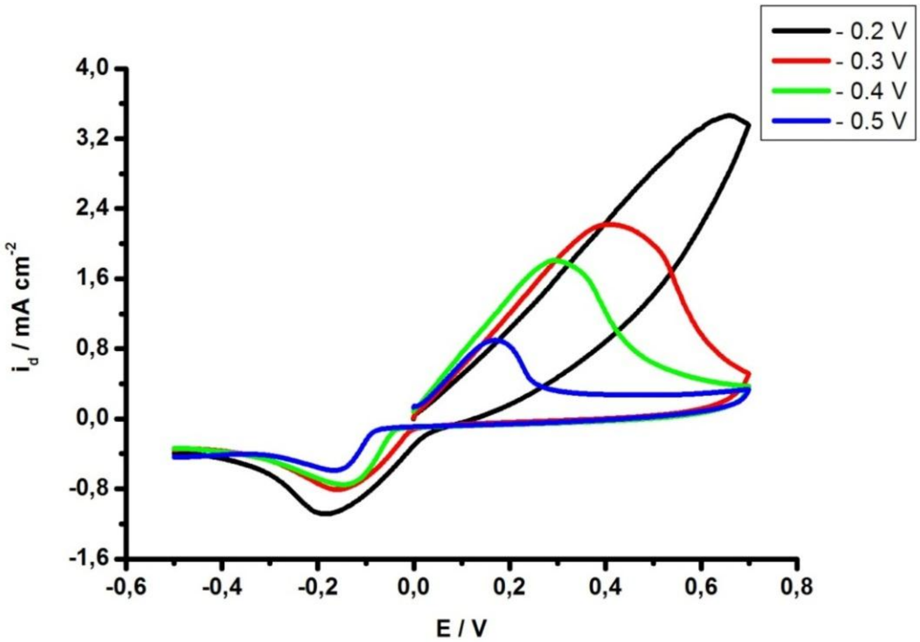

Figure 3.14 CV measurements of substrate having 50 mC/cm^{-2} silver charge density in 0.1 M $LiClO_4$ dissolved in ACN at 50 mV/s vs. Ag wire.

Detailed examination of Figures 3.9-3.14 reveals that the effect of reduction potential on reduced silver amount on the polymer surface can be observed since the amount of reduced silver particles onto polymer can be calculated easily by the area under the curve. Figure 3.9 shows that, when 2.5 mC/cm^2 silver was reduced onto polymer electrochemically, no matter what the voltage was, almost the same amount of silver was reduced onto PEDOT coated ITO glass. However, when reduced silver amount was increased to 5, 7.5, 10, 25, and 50 mC/cm^2, the amount of silver on the surface of the polymer was decreased at higher voltage values. The reason of this decrease can be that the fast reduction of silver ions at lower voltage values provides reduction of silver particles with different morphologies and smaller sized onto polymer compared to higher voltage values (Figure 3.15, Figure 3.16).

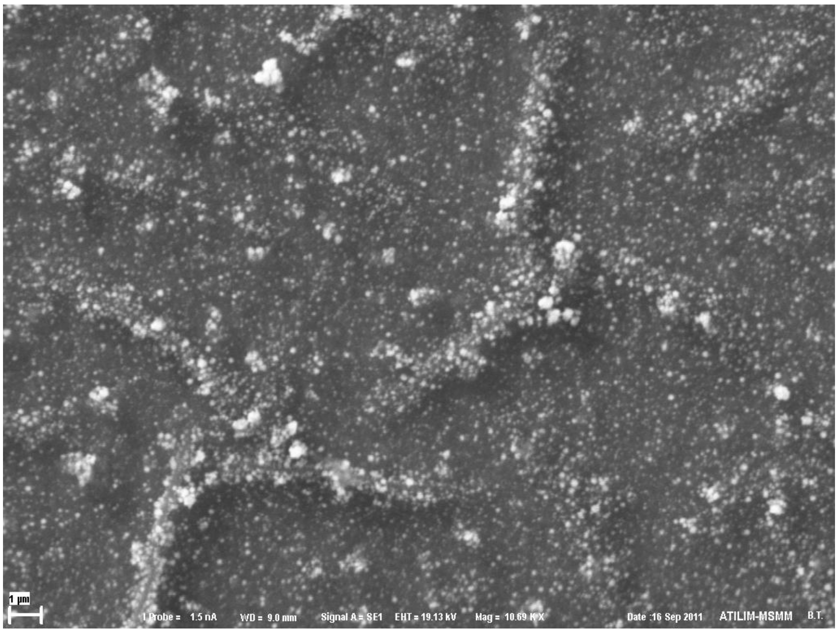

Figure 3.15 SEM image of substrate prepared by applying -0.5 V in 0.002 M $AgNO_3$ dissolved in 0.1 M $LiClO_4$/ACN.

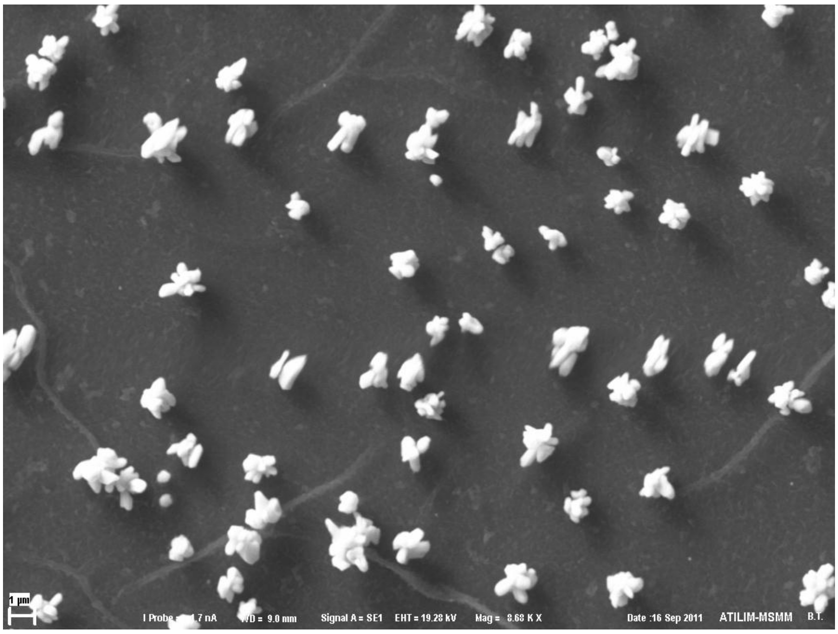

Figure 3.16 SEM image of substrate prepared by applying -0.2 V in 0.002 M $AgNO_3$ dissolved in 0.1 M $LiClO_4$/ACN.

3.2.1.1 Optimization of Scan Rate

The CV measurements were taken at different scan rates for optimization; 25, 50, 75, and 100 mV/s values were performed. The results are given in Figure 3.17.

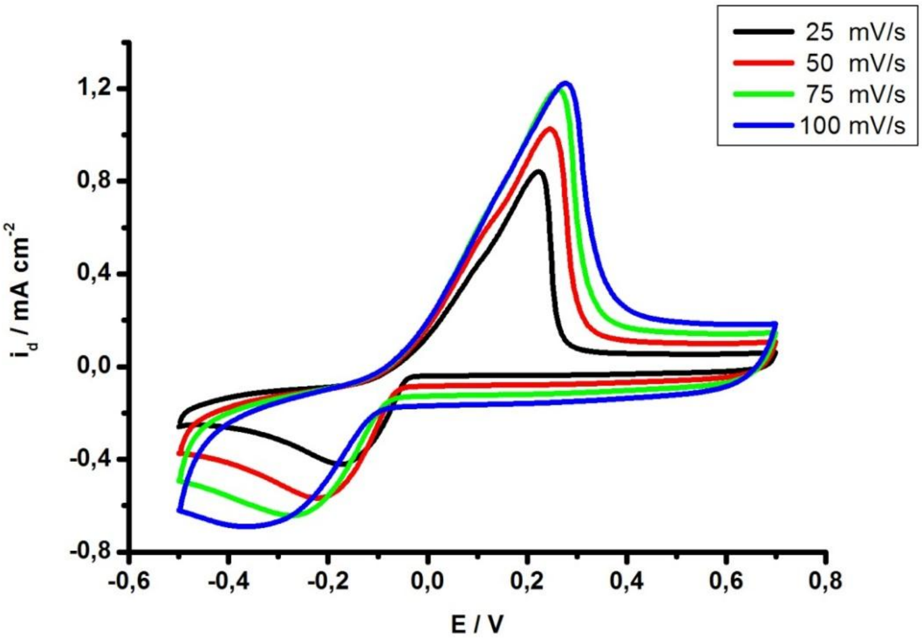

Figure 3.17 CV measurements of substrate at different scan rates; 25, 50, 75, 100 mV/s in 0.002 M $AgNO_3$ dissolved in 0.1 M $LiClO_4$/ACN vs. Ag wire.

When Figure 3.17 was examined, two scan rates, 25 mV/s and 50 mV/s, can be selected as optimum values, since the reduction peak of silver can be more clearly defined at these rates. 50 mV/s was selected as an optimum value due to its time saving advantage during the experiments.

3.2.2 Optimization of Silver Ion Concentration

The concentrations of $AgNO_3$ were varied to $1.0x10^{-3}$, $2.0x10^{-3}$, $5.0x10^{-3}$, $1.0x10^{-2}$ M. The intensities of SERS spectrum of 10^{-7} M BCB were compared shown in Figure 3.18. Silver ion concentration plays an important role during reduction of silver ions onto the polymer surface.

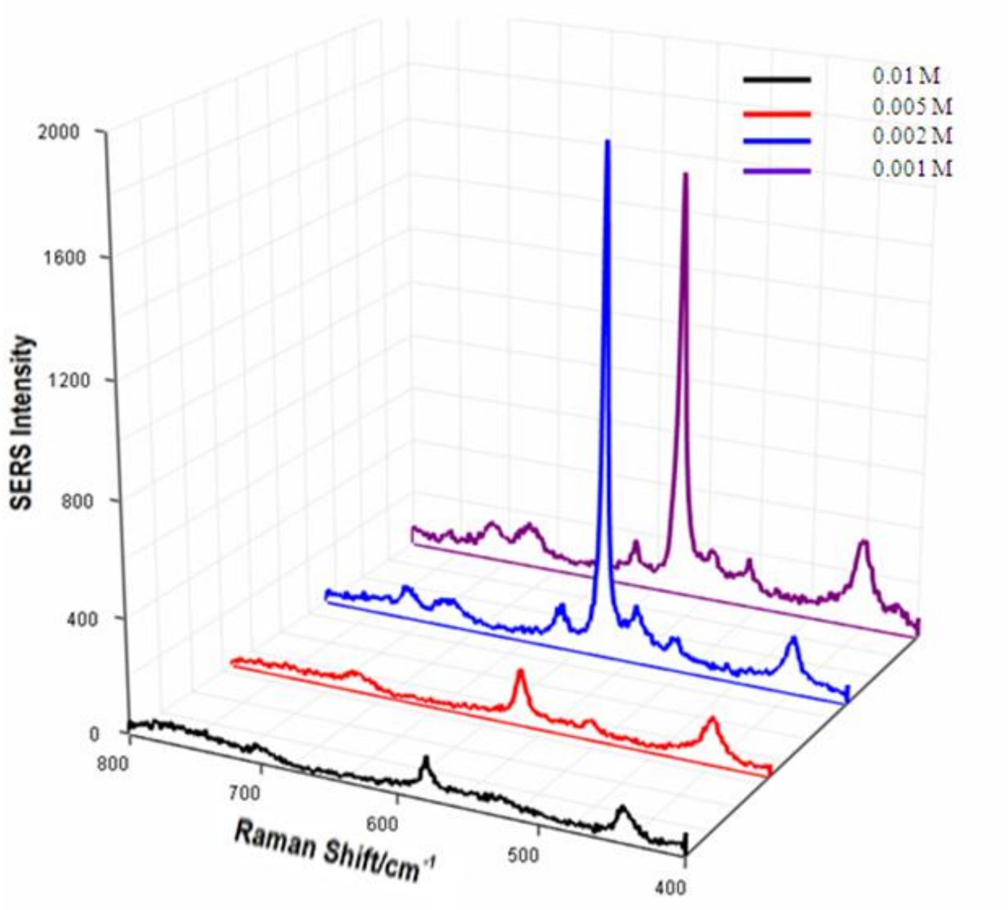

Figure 3.18 SERS measurements of substrates prepared with different concentrations of silver.

In Figure 3.18, it is seen that the highest enhancement in Raman signal is observed when the concentration of silver ions in the electrolyte solution was 0.002 M. The use of more concentrated silver ions in the solution results in a sharp decrease in SERS signals. However, almost fifty percent dilution in the concentration causes only a five percent decrease in the signal. It seems that at lower concentration of silver, reduction rate decreases which possibly causes a more homogeneous accumulation of the particles (Figures 3.19-3.22).

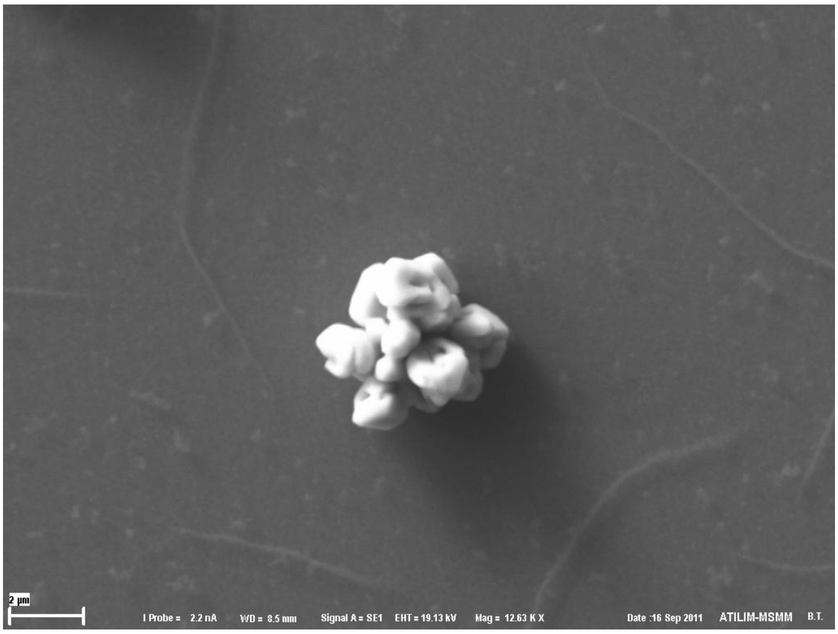

Figure 3.19 SEM image of substrate prepared by using 0.01 M $AgNO_3$ dissolved in 0.1 M $LiClO_4$/ACN.

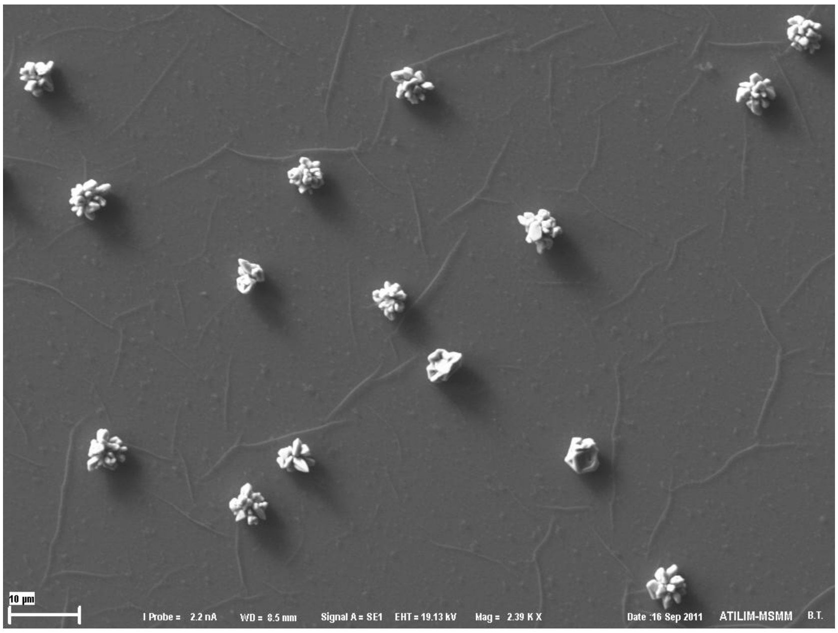

Figure 3.20 SEM image of substrate prepared by using 0.01 M $AgNO_3$ dissolved in 0.1 M $LiClO_4$/ACN.

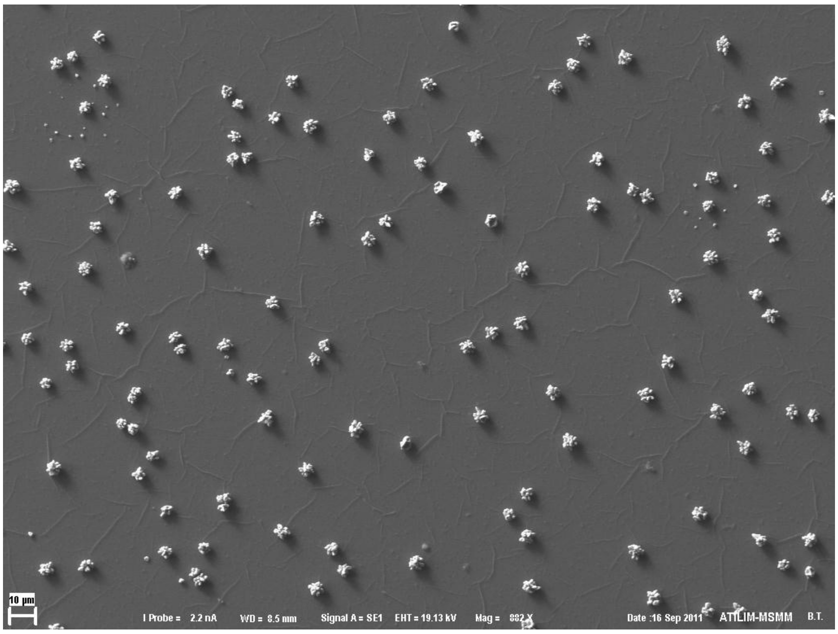

Figure 3.21 SEM image of substrate prepared by using 0.01 M $AgNO_3$ dissolved in 0.1 M $LiClO_4$/ACN.

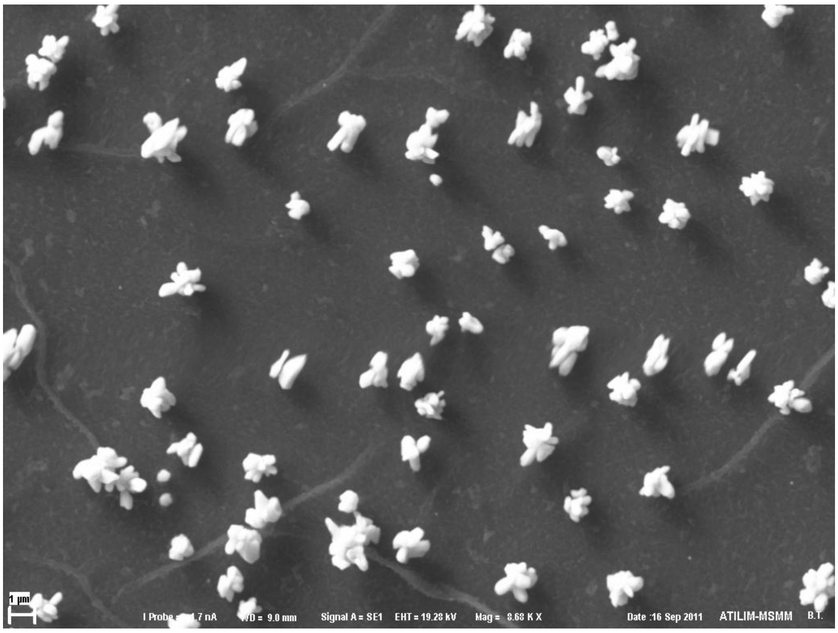

Figure 3.22 SEM image of substrate prepared by using 0.002 M $AgNO_3$ dissolved in 0.1 M $LiClO_4$/ACN.

3.2.3 Optimization of Polymer Film Thickness

In this section, polymer film thickness was optimized in order to obtain ideal substrate. To change the thickness of coated polymer film, different charge densities; 10, 20, and 30mC/cm^2 were applied to electrolysis cell. During this optimization, charge density of silver was kept constant at 50 mC/cm^2. Prepared substrates were tested in terms of their SERS activity (Figure 3.23).

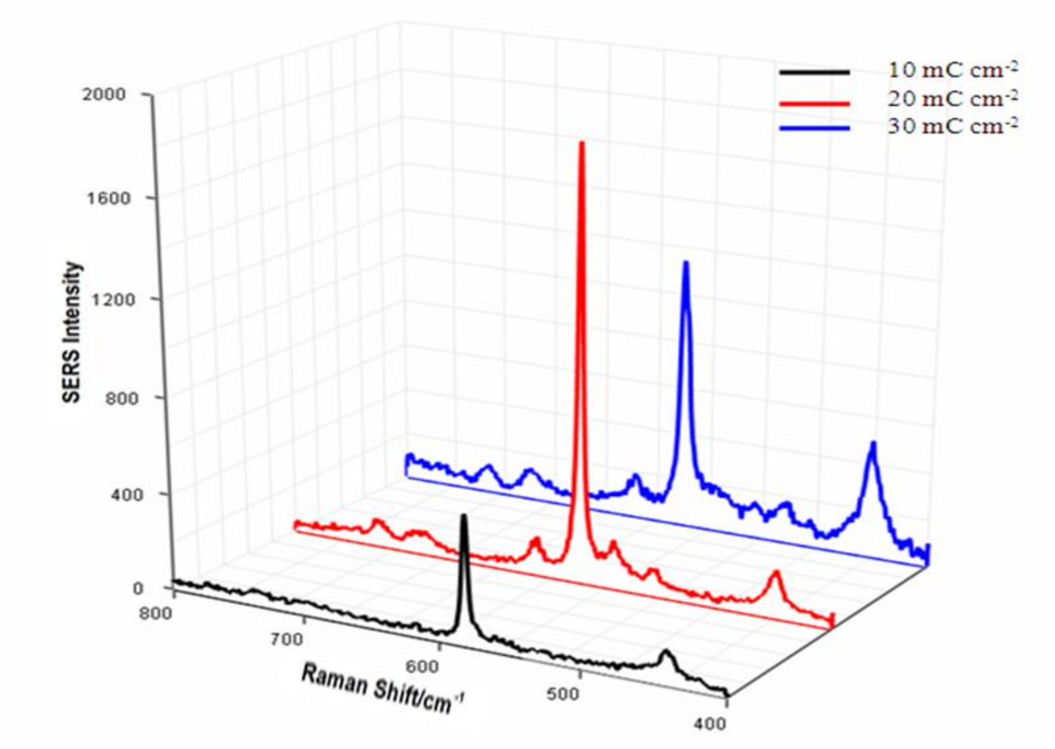

Figure 3.23 SERS measurements of substrates having different amounts of the PEDOT polymer.

As shown in Figure 3.23, the highest signal is acquired with a PEDOT coating having the medium thickness (20 mC/cm^2 charge density). The SERS signal obtained with thicker PEDOT polymer (30 mC/cm^2 charge density) is greater than that of the thinner one (10 mC/cm^2 coating). One possible reason can be the increase in the conductance of the surface when the film thickness gets thinner. Hence reduction rate is increased and relatedly the size of the reduced silver particles becomes greater compared to the ones in thicker coatings. The SEM images of the particles prepared with a charge density of 10 mC/cm^2 and 20 mC/cm^2 are given in Figure 3.24 and Figure 3.25.

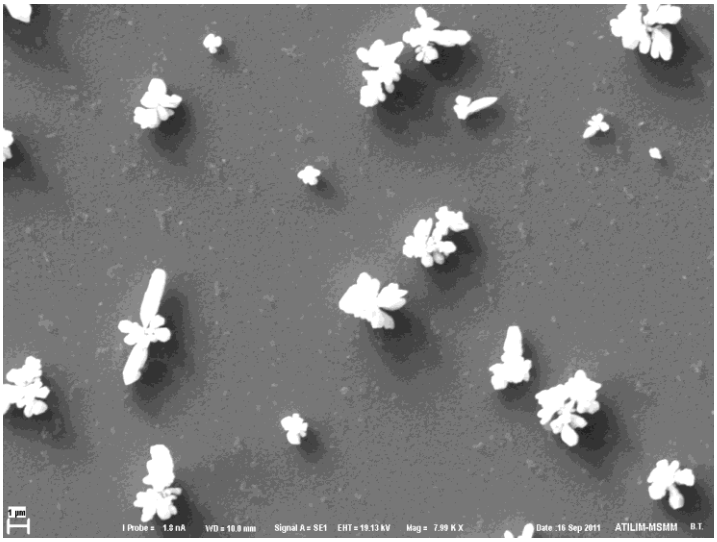

Figure 3.24 SEM image of the substrate prepared with 10 mC/cm^2 PEDOT and 50 mC/cm^2 silver.

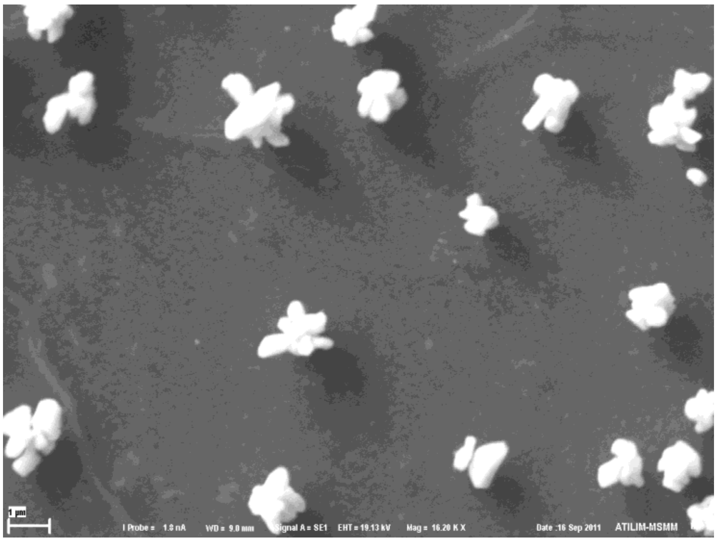

Figure 3.25 SEM image of the substrate prepared with 20 mC/cm^2 PEDOT and 50 mC/cm^2 silver.

Control of the morphology of a nanostructure is a difficult task. The growing processes are always proceeding through an energetically available facet. As can be seen from Figure 3.24, when the deposition is performed on a thin polymer film, numerous nonuniform flowerlike crystals have been obtained on the electrode surface. All the nonuniform side branches grow from one or several adjacent centers to various directions.

The SEM image of the substrate which has been given the highest SERS signal enhancement (20mC/cm^2, polymer charge density) is depicted in Figure 3.25. Although silver amount was the same in all of these preparations, slow reduction of the silver due to the conduction of the charge through the polymer makes the difference in the accumulation of the particles on the surface. Compared to Figure 3.24, it seems that the growth of the silver on the surface takes place in such a way that the silver blocs having smooth surfaces are piled up on top of each other. It is known that, electromagnetic enhancement is the key factor for obtaining high SERS enhancement. Probably, the arrangement shown in Figure 3.25 provides the highest overlap among the surface plasmons of these discrete silver blocs at each accumulation. Further increase in the charge density of PEDOT (30 mC/cm^2, polymer charge density) probably reduces the conductance of surface and the accumulation type changes entirely. Unfortunately, SEM image of this surface could not be taken because of the thick polymer coating which was burned wherever the objective was focused on.

3.2.4 Optimization of Silver Amount

The amount of silver reduced onto polymer surface can be increased by increasing the charge density of reduced silver particles. This is clearly seen from Figure 3.26 that when the charge intensity of reduced silver is increased, the amount of silver oxidized during CV measurements was increased, too. This was an expected result. In addition, for 50 mC/cm^2 silver coated surface, all of the reduced silver particles could not be oxidized in a single CV cycle. In the second cycle, however, almost all of reduced silver particles are oxidized from the surface of the polymer (Figure 3.27).

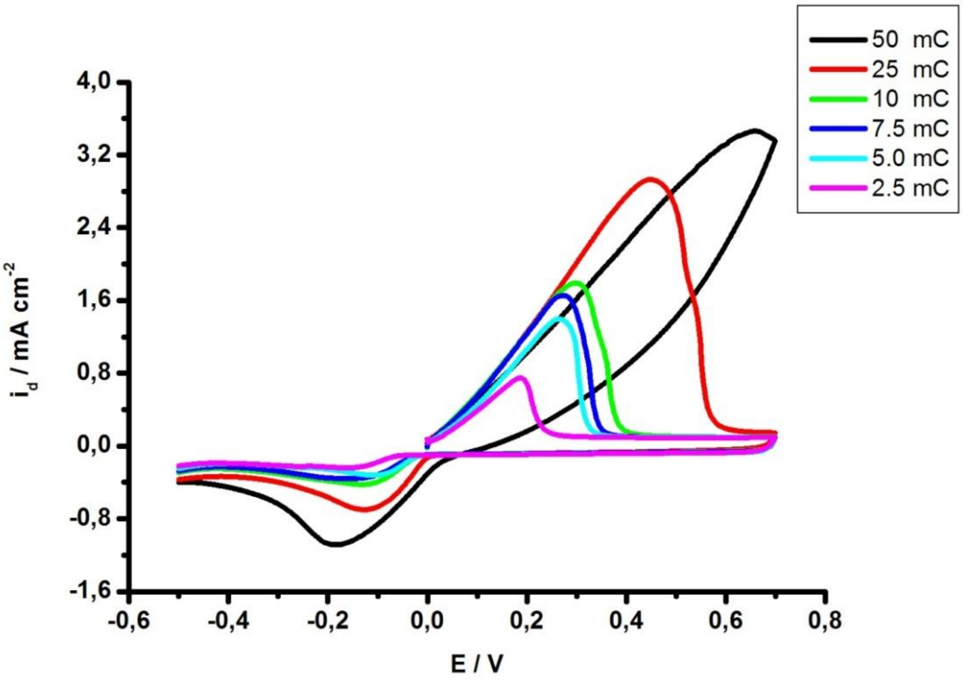

Figure 3.26 CV measurements of substrates having different silver charge densities in 0.1 M $LiClO_4$ dissolved in ACN at 50 mV/s vs. Ag wire.

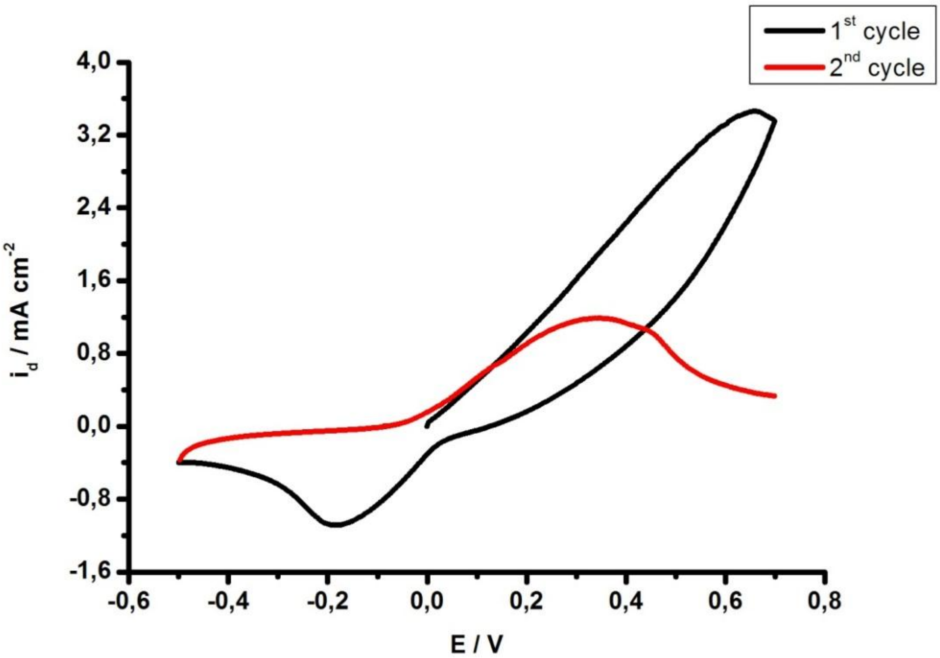

Figure 3.27 CV measurement of substrate having 50 mC silver charge density in 0.1 M $LiClO_4$ dissolved in ACN at 50 mV/s vs. Ag wire.

Charge density of the silver was optimized in order to increase the SERS enhancement. The charge densities of the silver were 10, 30, 40, 50, 60, and 70 mC/cm^2. During this optimization, charge density of polymer deposition was kept constant at 20 mC/cm^2, determined from the previous studies. Prepared substrates were tested in terms of their SERS activity (Figure 3.28).

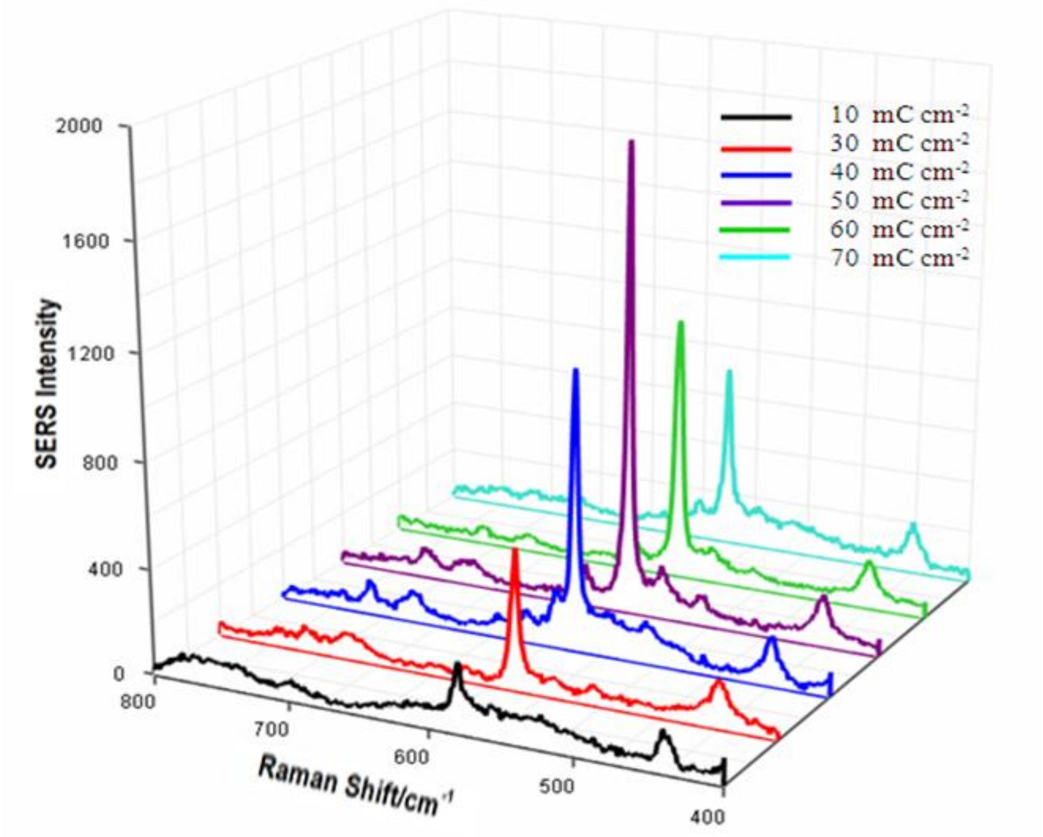

Figure 3.28 SERS measurements of substrates having different amount of silver.

It is known that SERS signal enhancement is proportional with the number of silver particles causing SERS enhancement. Accordingly, lower amounts of silver resulting fewer silver particles; thus, causing lower SERS signals (Figure 3.28). As expected, by increasing silver amount, number of silver particles was increased (Figure 3.30). Therefore, SERS performance of substrates increased up to 50 mC/cm^2 silver amount. Exceeding this value reduced signal intensities.

SEM images of the substrates prepared with various (10, 50 and 70 mC/cm^2) silver charge densities at a fixed PEDOT charge density of 20 mC/cm^2 are shown an Figure 3.29-3.31.

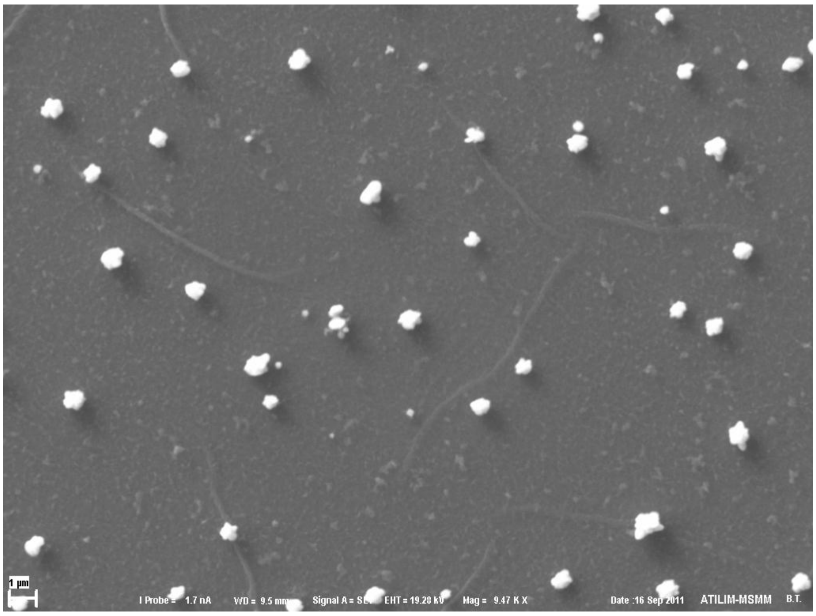

Figure 3.29 SEM image of the substrate prepared with 10 mC/cm^2 Ag and 20 mC/cm^2 PEDOT.

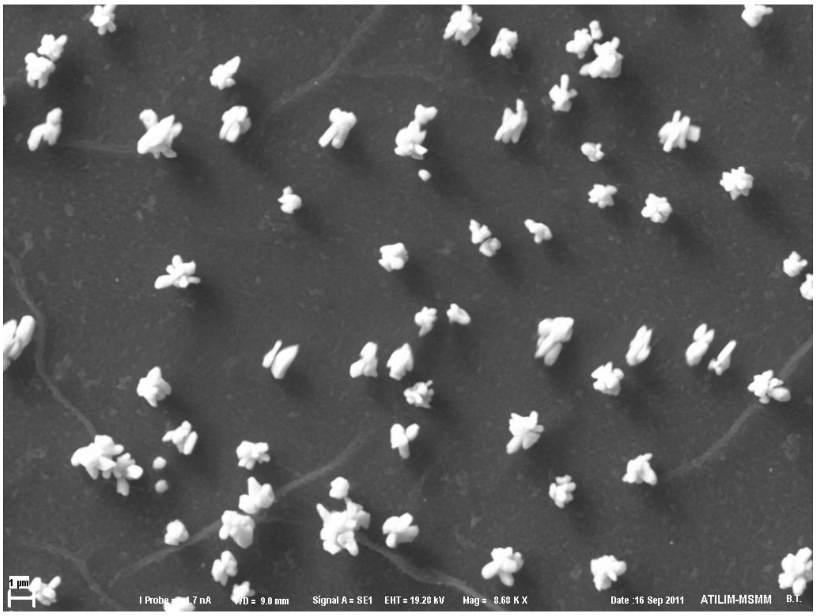

Figure 3.30 SEM image of the substrate prepared with 50 mC/cm^2 Ag and 20 mC/cm^2 PEDOT.

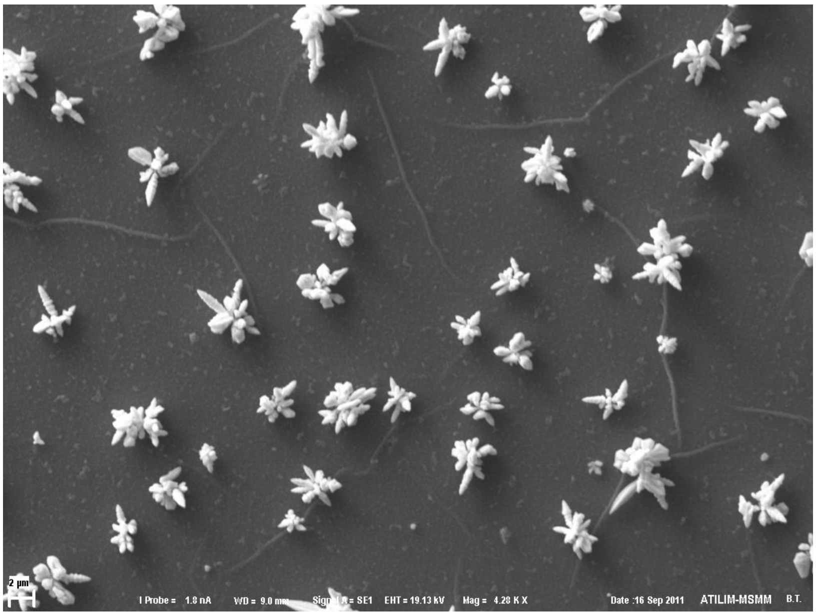

Figure 3.31 SEM image of the substrate prepared with 70 mC/cm^2 Ag and 20 mC/cm^2 PEDOT.

As expected the lowest number of nucleation center is observed from the surface prepared by using the lowest amount of silver charge density (10 mC/cm^2), Figure 3.29. The number of accumulation centers is increased when 50 mC/cm^2 charge density is applied in the substrate preparation (Figure 3.30). Further increase in the charge density of silver causes growth of the particles rather than the initiation of new nucleation centers (Figure 3.31). Therefore after this point, the morphology of the particles which determines the establishment of the electromagnetic field around silver accumulation centers becomes important. The SEM images are supporting this conclusion. If the SEM image (Figure3.31) of the surface prepared with a silver charge density of 70 mC/cm^2 is compared with the one (Figure3.23) that was prepared with a PEDOT charge density of 10 mC/cm^2, the very same flowerlike silver particle formations can be seen easily. The SERS activity of these surfaces are lower than the ones prepared with the mentioned optimum values (charge density of silver and PEDOT are 50 mC/cm^2 and 20 mC/cm^2).

3.3 Properties of the PEDOT-Ag Surface as a SERS Substrate

After optimizing the parameters for the preparation of a robust SERS substrate, the homogeneity and the shelf life of the substrates were investigated. Homogeneity is very crucial in terms of quantitative SERS applications.

3.3.1 Homogeneity of the SERS Substrates

The reproducibility of the SERS signals depends on the homogeneous distribution of the metal providing the plasmons on the substrate surface. In order to overcome inhomogeneous silver reduction onto polymer causing irreproducible signals, as experienced in a previous study (Köksel, 2009), PEDOT film was used as the supporting material for homogeneous silver particles formation on the polymer since, EDOT monomer polymerizes regularly, i.e., well-oriented like a spider web. To test the homogeneity of the substrate, SERS measurements of 10^{-7} M BCB were acquired at different points on the same substrate (Figure 3.32).

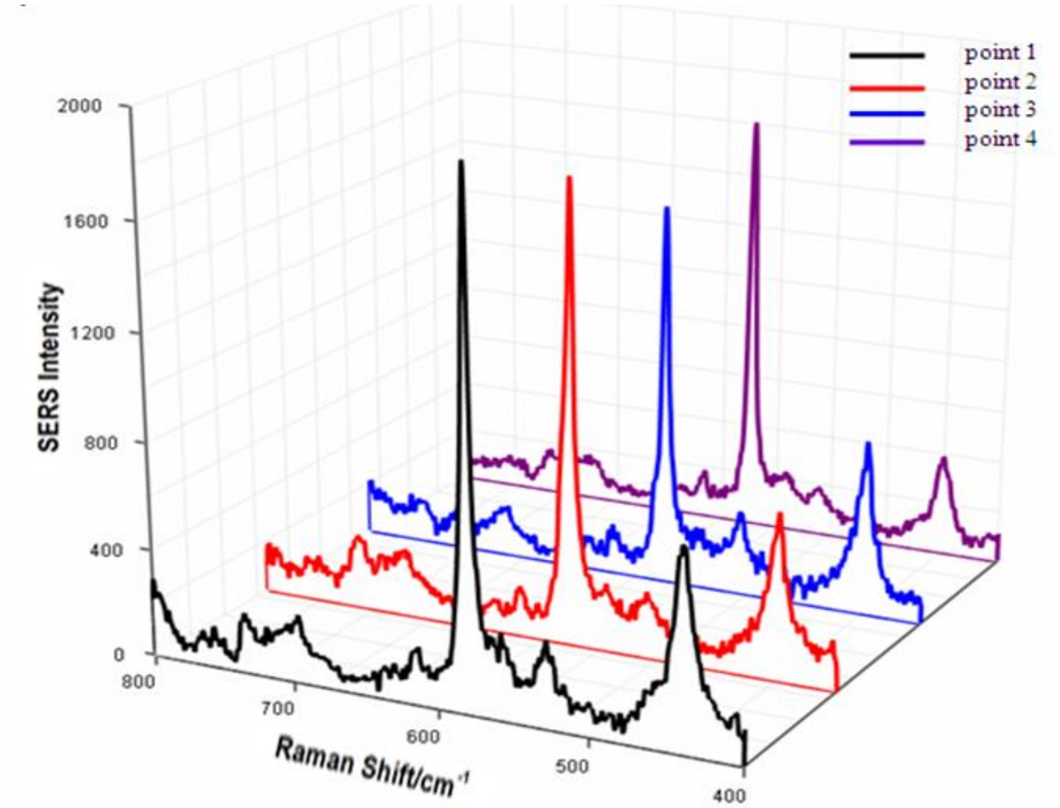

Figure 3.32 Raman spectrum of 10^{-7} M BCB at different points of PEDOT-Ag substrate.

The point to point reproducibility of the SERS spectra on the same substrate was tested by calculating the CV% of the peak intensities at around 580 cm^{-1} by taking the average of four SERS spectra. The CV% value was calculated as 9.34%. The reproducibility of the signals obtained from the same substrate or different substrates prepared in the same way is usually not mentioned in most of the studies. Therefore, the comparison with the literature values could not be done. However, this issue is becoming important due to the increased usage of SERS in quantitative analysis.

3.3.2 Stability of the SERS Substrates

For SERS applications, the stability of the substrate is one of the key parameter. For this reason, the stability of PEDOT-Ag film was investigated by taking Raman spectrum of 10^{-6} M BCB at different time periods (Figure 3.33). From Figure 3.33, it is seen that in one month time, signal intensities stayed almost the same. The possible reason of the slight decreasing can be the oxidation of a small number of silver particles on the surface. Therefore, the numbers of silver particles causing surface plasmons decreased, lowering SERS performance of substrate. The oxidation problem of SERS substrates prepared utilizing silver nanostructures is a well-known problem. Based on this long shelf life of one month, it can be concluded that the presence of the polymer around the silver particles preserve it from the air oxidation. If the substrates were kept in a desiccator under inert nitrogen atmosphere, this duration can be extended more.

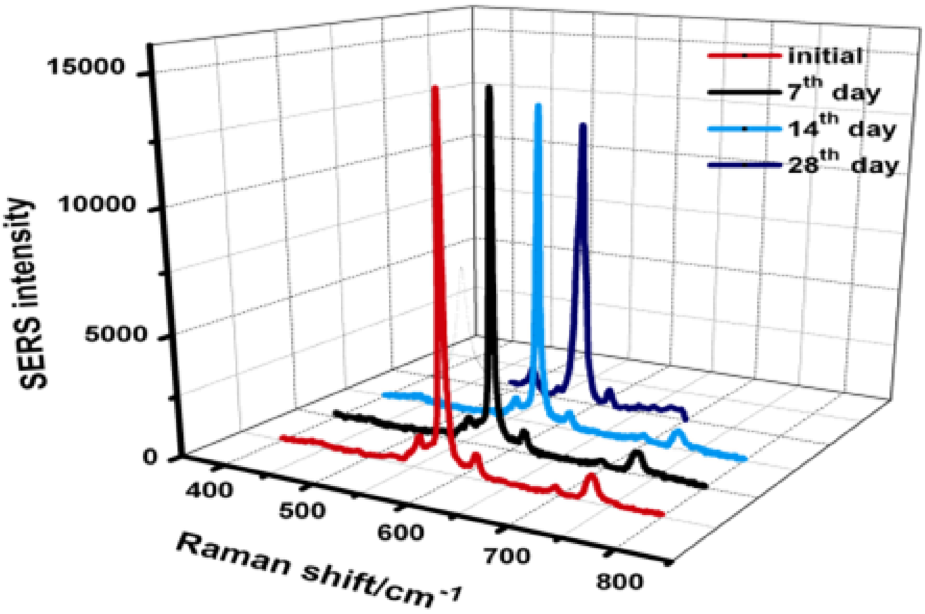

Figure 3.33 Raman spectrum of 10^{-6} M BCB at different times on PEDOT-Ag substrate.

3.4 The Use of Substrates in SERS Detection of R6G and 4-MBA

SERS spectrum of 10^{-5} M R6G is taken (Figure 3.34). The peak at 1188 cm^{-1} is related with C-C stretching vibrations, while the peaks at 1303, 1356, and 1575 cm^{-1} are related with aromatic C-C stretching vibrations (Yeo, Schmid, Zhang, & Zenobi, 2007).

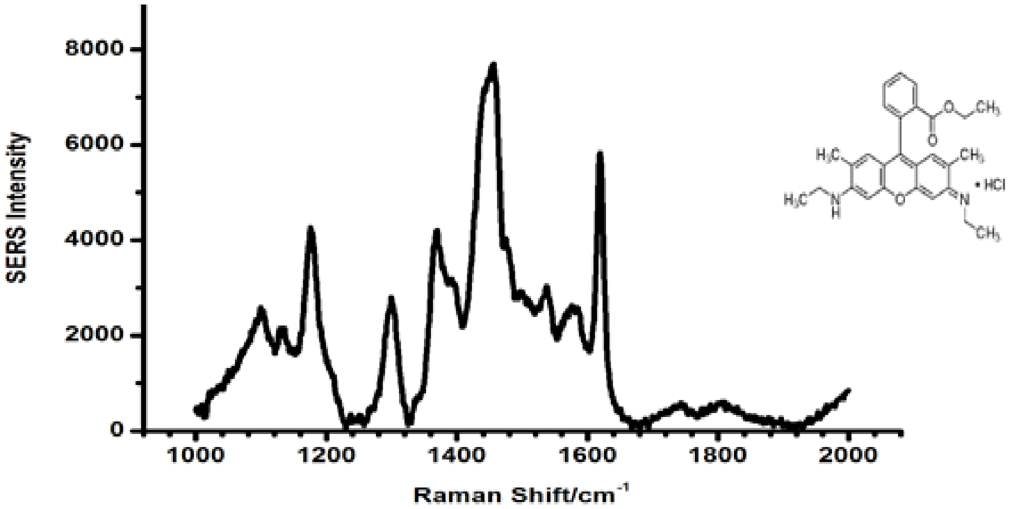

Figure 3.34 Raman spectrum of 10^{-5} M R6G on PEDOT-Ag substrate.

SERS spectrum of 10^{-4} M 4-MBA is taken (Figure 3.35). The peaks at 1073 and 1583 can be used for the detection of 4-MBA. These strong bands have been assigned to aromatic ring vibrations (Michota & Bukowska, 2003).

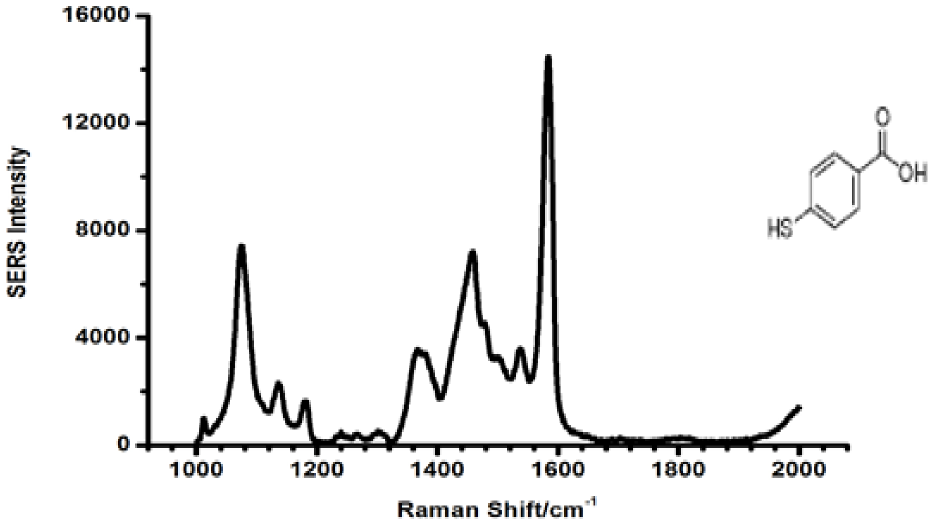

Figure 3.35 Raman spectrum of 10^{-4} M 4-MBA on PEDOT-Ag substrate.

CHAPTER 4

CONCLUSION

Main purpose of this study is to prepare a new SERS active substrate which is homogeneous, stable, and providing high Raman signal enhancement. This substrate is prepared by using electrochemical method.

To provide homogeneity and stability, PEDOT polymer is used since PEDOT polymerizes regularly and it is very stable polymer.

To provide high SERS enhancement many optimizations were performed. Polymer amounts, silver amounts, silver reduction potential, and silver ion concentration were optimized to get high SERS response from chemicals.

To find optimum values many substrates were prepared and most of them are investigated by using CV, SEM, UV-Vis, and Raman spectroscopy techniques.

After optimization, homogeneity and stability properties of the substrate were investigated. To investigate homogeneity property, SERS spectra were taken from different points of the same substrate. To investigate stability property, SERS spectra were taken at different time periods.

After investigation of the substrate properties, R6G and 4-MBA chemicals were detected by using the prepared substrates.

REFERENCES

ACS. Retrieved August 20, 2011, from ACS: http://portal.acs.org/portal/acs/corg/content?_nfpb=true&_pageLabel=PP_ARTICLEMAIN&node_id=924&content_id=WPCP_007605&use_sec=true&sec_url_var=region1&__uuid=48104621-952f-4eb8-abde-df5643f191b8

Albrecht, M. G., & Creighton, J. A. (1977). Anomalously Intense Raman-Spectra of Pyridine at a Silver Electrode. *Journal of American Chemical Soceity, 99*, 5215-5217.

Arunkumar, K. A., & Bradley, E. B. (1983). Theory of Surface Enhanced Raman Scattering. *Journal of Chemical Physics, 78,* 2882-2888.

Asavapiriyonont, S., Chandler, G. K., Pletcher, G. A., & Gunawardena, D. (1984). The Electrodeposition of Polypyrrole Films from Aqueous Solutions. *Journal of Electroanalytical Chemistry, 177,* 229-244.

Burroughes, J. H., Bradley, D. D., Brown, A. R., Marks, R. N., MacKay, K., Friend, R. H., et al. (1990). Light-Emitting Diodes Based on Conjugated Polymers. *Nature, 347*, 539-541.

Campion, A., & Kambhampati, P. (1998). Surface-enhanced Raman scattering. *Chemical Society Reviews, 27*, 241-250.

Campion, A., Ivanecky, J. E., Child, C. M., & Foster, M. (1995). On the Mechanism of Chemical Enhancement in Surface-Enhanced Raman Scattering. *Journal of American Chemical Society, 117*, 11807-11808.

Chen, X., Jeon, Y.-M., Jang, J.-W., Qin, L., Huo, F., Wei, W., et al. (2008). On-Wire Lithography-Generated Molecule-Based Transport Junctions: A New Testbed for Molecular Electronics. *Journal of American Chemical Society, 130,* 8166-8168.

Chiang, C., Fincher, C., Park, Y., Heeger, A., Shirakawa, H., Louis, E., et al. (1977). Electrical Conductivity in Doped Polyacetylene. *Physical Review Letters, 39,* 1098-1101.

Chiang, C., Park, Y., Heeger, A., Shirakawa, H., Louis, E., & A.G., M. (1978). Conducting polymers: Halogen doped polyacetylene. *Journal of Chemical Physics, 69*, 5098-5104.

Christou, K., Knorr, I., Ihlemann, J., Wackerbarth, H., & Beushausen, V. (2010). Fabrication and Characterization of Homogeneous Surface-Enhanced Raman Scattering Substrates by Single Pulse UV-Laser Treatment of Gold and Silver Films. *Langmuir, 26*, 18564–18569.

Chuang, Liu, Y. C., & Thomas, C. (2003). Self-Assembly and Autopolymerization of Pyrrole and Characteristics of Electrodeposition of Polypyrrole on Roughened Au(111) Modified by Underpotentially Deposited Copper. *The Journal of Physical Chemistry B, 107*, 9802–9807.

College of Chemistry. Retrieved August 11, 2011, from College of Chemistry: http://www.cchem.berkeley.edu/ramgrp/alpha/people/Alumni/phil/index.html

Desbene-Monvernay, A., Lacaze, P. C., & Dubois, J. E. (1981). Polaromicrotribometric (PMT) and IR, ESCA, EPR Spectroscopic Study of Colored Radical Films Formed by the Electrochemical Oxidation of Carbazoles: Part I. Carbazole and N-ethyl, N-phenyl and N-carbazyl Derivatives. *Journal of Electroanalytical Chemistry, 129*, 229-241.

Diaz, A. F., Kanazawa, K. K., & Gardini, G. P. (1979). Electrochemical polymerization of pyrrole. *Chemmical Communications, 10*, 635-636.

El-Sayed, Nikoobakht, B., & Mostafa, A. (2003). Surface-Enhanced Raman Scattering Studies on Aggregated Gold Nanorods. *The Journal of Physical Chemistry A, 107*, 3372–3378.

Fleischmanna, M., Hendraa, P., & McQuillana, A. (1974). Raman spectra of pyridine adsorbed at a silver electrode. *Chemical Physics Letters, 26*, 163-166.

Freeman, R. G., Grabar, K. C., Allison, K. J., Bright, R. M., Davis, J. A., Guthrie, A. P., et al. (1995). Self-Assembled Metal Colloid Monolayers: An Approach to SERS Substrates. *Science, 267*, 1629-1632.

Gandini, A., & Belgancem, M. N. (1997). Nanomaterials: synthesis, properties, and applications. *Progress in Polymer Science, 22*, 1203.

Gaupp, C. L. (2002). Structure-Property Relationships of Electrochromic 3,4-alkylenedioxy Heterocycle-Based Polymers and Copolymers. University of Florida.

Genius, E., Bidan, G., & Diaz, A. F. (1983). Spectroelectrochemical Study of Polypyrrole Films . *Journal of Electroanalytical Chemistry, 149*, 101-113.

Germain, V., Brioude, A., Ingert, D., & Pileni, M. P. (2005). Silver Nanodisks: size selection via centrifugation and optical properties. *Journal of Chemical Physics, 122*, 124707-124715.

Goel, A., Dixit, M., Chaurasia, S., Kumar, A., Raghunandan, R., Maulik, P. R., et al. (2008). Vapor-Phase Processable Novel Nonplanar Donor−Acceptor Quateraryls for Blue OLEDs. *Organic Letters, 10*, 2553-2556.

İçli Özkut, M. (2011). Color Engineering of π-Conjugated Donor-Acceptor Systems: The Role of Donor and Acceptor Units on The Neutral State Color. Middle East Technical University.

Ingle, J. D., & Crouch, S. (1988). *Spectrochemical Analysis.* Englewood Cliffs, New Jersey: Prentice Hall.

Inzelt, G. (2008). *Conducting polymers: A New Era in Electrochemistry.* Heidelberg: Springer.

Jain, P., Huang, I. H., & El-Sayed, M. (2007). Review of some interesting surface plasmon resonance-enhanced properties of noble metal nanoparticles and their applications to biosystems. *Plasmonics, 2*, 107-118.

Jeanmarie, D. C., & Van Duyne, R. P. (1977). Surface Raman Spectroelectrochemistry .1. Heterocyclic, Aromatic, and Aliphatic-Amines Adsorbed on Anodized Silver Electrode. *Journal of Electroanalytical Chemistry and Interfacial Electrochemistry, 84*, 1-20.

Jonas, F., & Schrader, L. (1991). Conductive Modifications of Polymers with Polypyrroles and Polythiophenes. *Synthetic Metals, 41*, 831-836.

Kneipp, K., Kneipp, H., Deinum, G., Itzkan, I., Dasari, R. R., & Feld, M. S. (1998). Single-molecule detection of a cyanine dye in silver colloidal solution using near-infrared surface-enhanced Raman scattering. *Applied Spectroscopy, 52*, 175-178.

Kneipp, K., Kneipp, H., Itzkan, I., Dasari, R. R., & Feld, M. S. (1999). Surface-enhanced non-linear Raman scattering at the single- molecule level. *Chemical Physics, 247*, 155-162.

Kneipp, K., Kneipp, H., Kartha, V. B., Manoharan, R., Deinum, G., Itzkan, I., et al. (1998). Detection and identification of a single DNA base molecule using surface-enhanced Raman scattering (SERS). *Physical Review E, 57,* R6281-R6284.

Kneipp, K., Kneipp, H., Manoharan, R., Itzkan, I., Dasari, R. R., & Feld, M. S. (1998). Near-infrared surface-enhanced Raman scattering can detect single molecules and observe 'hot' vibrational transitions. *Journal of Raman Spectroscopy, 29*, 743-747.

Kneipp, K., Wang, Y., Kneipp, H., Perelman, L. T., Itzkan, I., Dasari, R. R., et al. (1997). Single molecule detection using surface-enhanced Raman scattering (SERS). *Physical Review Letters, 78,* 1667-1670.

Le Ru, E., Blackie, E., & Etchegoin, P. (2007). Surface enhanced Raman Scattering Enhancement factors: A Comprehensive study. *Journal of Physical Chemistry C, 111,* 13794-13803.

Lee, I., Han, S. W., & Kim, K. (2001). Simultaneous preparation of SERS-active metal colloids and plates by laser ablation. *Journal of Raman Spectroscopy, 32,* 947-952.

Liscio, A., De Luca, G., Nolde, F., Palermo, V., Müllen, K., & Samori, P. (2008). Photovoltaic charge generation visualized at the nanoscale: A proof of principle. *Journal of American Chemical Society, 130,* 780-781.

Liu, Y. (2004). Enhancement in the Raman Scattering of Polypyrrole Electrodeposited on Roughened Gold. *The Journal of Physical Chemistry B, 108,* 2948-2952.

Liu, Y. C., Yu, C. C., & Sheu, S. F. (2006). Improved surface enhanced Raman scattering on optimum electrochemically roughened silver substrates. *Analytica Chimica Acta, 577*, 271-275.

Long, D. A. (2002). *Raman Effect: A Unified Treatment of Raman Scattering by Molecules.* Chichester, New York: Wiley.

Lu, Z., Ruan, W., Yang, J., Xu, W., Zhao, C., & Zhao, B. (2008). Deposition of Ag nanoparticles on porous anodic alumina for surface enhanced Raman scattering substrate. *Journal of Raman Spectroscopy, 40,* 112-116.

MacDiarmid, A. G., & Epstein, A. J. (1989). Polyanilines: A Novel Class of Conducting Polymers. *Faraday Discussions of the Chemical Society, 88,* 317-333.

Maxwell, D. J., Emory, S., & Nie, S. (2001). Nanostructured Thin-Film Materials with Surface-Enhanced Optical Properties. *Chemistry of Materials*, *13*, 1082-1088.

McCreery, & Richard, L. (2000). *Raman Spectroscopy for Chemical Analysis.* New York: Wiley.

Michota, A., & Bukowska, J. (2003). Surface-Enhanced Raman Scattering (SERS) of 4-mercaptobenzoic Acid on Silver and Gold Substrates. *Journal of Raman Spectroscopy, 34*, 21-25.

Movasaghi, Z., Rehman, S., & Rehman, I. U. (2007). Raman spectroscopy of biological tissues. *Applied Spectroscopy Rewievs, 42*, 493-541.

Murphy, C. J., Gole, A. M., Hunyadi, S. E., Stone, J. W., Sisco, P. N., Alkilany, A., et al. (2008). Chemical sensing and imaging with metallic nanorods. *Chemical Communications, 5*, 544-557.

Nie, S. M., & Emory, R. S. (1997). Probing single molecules and single nanoparticles by surface-enhanced Raman scattering. *Science, 275*, 1102-1106.

Open Library. Retrieved August 15, 2011, from Open Library: http://openlibrary.org/books/OL14028951M/Molecular_diffraction_of_light.

Orendorff, C. J., Gearheart, L., Jana, N. R., & Murphy, C. J. (2006). Aspect ratio dependence on surface enhanced Raman scattering using silver and gold nanorod substrates. *Physical Chemistry Chemical Physics, 8*, 165-170.

Otto, A., Mrozek, I., Grabhorn, H., & Akemann, H. (1992). Surface-enhanced Raman scattering. *Journal of Physics: Condenced Matter, 4*, 1143-1212.

Park, H. K., Yoon, J. K., & Kim, K. (2006). Novel Fabrication of Ag Thin Film on Glass for Efficient Surface-Enhanced Raman Scattering. *Langmuir, 22*, 1626–1629.

Princeton Instruments. Retrieved August 17, 2011, from Raman Spectroscopy Basics: http://content.piacton.com/Uploads/Princeton/Documents/Library/UpdatedLibrary/Raman_Spectroscopy_Basics.pdf

Raman, C. V., & Krishnan, K. S. (1928). A New Type of Secondary Radiation. *Nature, 121*, 501-502.

Ritchie, R. H. (1957). Plasma Losses by Fast Electrons in Thin Films. *Pyhsical Review, 106*, 874-881.

Rupérez, A., & Laserna, J. J. (1996). Surface-enhanced Raman spectrometry of triamterene on a silver substrate prepared by the nitric acid etching method. *Talanta, 44*, 213-220.

Saagam. Retrieved August 16, 2011, from Saagam.com: http://saagam.com/info/alltimegreat/scitech/sir-cv-raman.php

Sanci, R., & Volkan, M. (2009). Surface Enhanced Raman Scattering Studies on Silve Nanorod Substrates. *Sensors and Actuators B: Chemical, 139*, 150-155.

Siemes, C., Bruckbauer, A., Goussev, A., Otto, A., Sinther, M., & Pucci, A. (2001). SERS-active sites on various copper substrates. *Journal of Raman Spectroscopy, 32*, 231–239.

Skoog, D., Holler, F., & Nieman, T. (1998). *Principles of Instrumental Analysis.* Orlando, Florida: Harcourt Brace & Company.

Smekal, A. (1923). Zur Quantentheorie der Dispersion. *Naturwissenschaften, 11,* 873-875.

Smith, H., & Denth, G. (2005). *Modern Raman Spectroscopy.* West Sussex: Wiley.

Stevenson, C. L., & Vo-Dinh, T. (1996). *Modern Tecchniques in Raman Spectroscopy.* West Sussex: Wiley.

Stiles, P., Dieringer, J., Shah, N., & Van Duyne, R. (2008). Surface-Enhanced Raman Spectroscopy. *Annual Review of Analytical Chemistry, 1,* 601–626.

Strobel, H. A., & Heineman, W. R. (1989). *Chemical Instrumentation: A Systematic Approach.* Massachusetts: Addison-Wesley Publishing Co.

Tourillon, G., & Garnier, F. J. (1982). New Electrochemically Generated Organic Conducting Polymers. *Journal of Electroanalytical Chemistry, 135*, 173-178.

Usta, H., Facchetti, A., & Marks, T. J. (2008). Air-Stable, Solution-Processable n-Channel and Ambipolar Semiconductors for Thin-Film Transistors Based on the Indenofluorenebis(dicyanovinylene) Core. *Journal of American Chemical Society, 130*, 8580-8581.

Venkata Raman - Biography. Retrieved August 17, 2011, from Nobelprize.org: http://nobelprize.org/nobel_prizes/physics/laureates/1930/raman-bio.html

Vo-Dinh, T. (1998). Surface-enhanced Raman spectroscopy using metallic nanostructures. *Trends in Analytical Chemistry, 17*(8-9), 557-582.

Vongsvivut, J., Robertsona, E. G., & McNaughtona, D. (2010). Surface-enhanced Raman spectroscopic analysis of fonofos pesticide adsorbed on silver and gold nanoparticles. *Journal of Raman Spectroscopy, 41*, 1137–1148.

Vosgröne, T., Meixner, A. J., Anders, A., Dietz, H., Sandman, G., & Plieth, W. (2004). Electrochemically deposited silver particles for surface enhanced Raman spectroscopy. *Surface Science, 597*, 102-109.

Vrije Universiteit. Retrieved August 15, 2011, from Vrije Universiteit: http://www.vub.ac.be/META/toestellen_raman.php?m=xpand&d=menu7

Wise, D. L., Wnek, G. E., Trantolo, D. J., Cooper, T. M., & Gresser, J. D. (1998). *Electrical and Optical Polymer Systems: Fundamentals, Methods, and Applications.* New York: Marcel Dekker Press.

Yang, K. H., Liu, Y. C., Hsu, T. C., & Juang, M. Y. (2009). New pathway to prepare surface enhanced Raman scattering active silver nanoparticles based on electrochemical methods. *Materials Letters*, *64*, 497-499.

Yeo, B., Schmid, T., Zhang, W., & Zenobi, R. (2007). Towards Rapid Nanoscale Chemical Analysis Using Tip-Enhanced Raman Spectroscopy with Ag-Coated Dielectric Tips. *Analytical Bioanalytical Chemistry, 387*, 2655–2662.

Yin, Y., Li, Z. Y., Zhong, Z., Gates, B., Xia, Y., & Venkateswaran, S. (2002). Synthesis and Characterization of Stable Aqueous Dispersions of Silver Nanoparticles Through the Tollens Process. *Journal of Materials Chemistry, 12*, 522-527.